

2-10
MIX

INSTITUTO GEOFISICO DEL PERU

RADIO OBSERVATORIO DE JICAMARCA

PROGRESS REPORT ON

COORDINATED SATELLITE AND INCOHERENT SCATTER OBSERVATIONS

Submitted to

NATIONAL AERONAUTICS AND SPACE ADMINISTRATION

Grant No. NGR-52-158-001

Principal Investigator: Dr. Ronald F. Woodman

Associate Researcher : Dr. C. Pablo Lagos



Reproduced by
NATIONAL TECHNICAL
INFORMATION SERVICE
US Department of Commerce
Springfield VA 22151

August 1971

FACILITY FORM 602	<u>N71-35437</u> (ACCESSION NUMBER)	<u>1</u> (THRU)
	<u>74</u> (PAGES)	<u>G3</u> (CODE)
	<u>12-121984</u> (NASA CR OR TMX OR AD NUMBER)	<u>13</u> (CATEGORY)

CONTENTS

	PAGE
ABSTRACT	1
Introduction	2
a) Electron Concentration and Temperature and Spread-F Measurements Co-ordinated with OGO-VI Passes	2
b) Electron Concentration and 6300 Å Nightglow Measurement	4
c) Special Events	5
Acknowledgement	6
References	7
Table I	8
APPENDIX I. Electron Density and Temperature Profiles Co-ordinated with OGO-VI Passes.	
APPENDIX II. Spread-F Observations Co-ordinated with OGO-VI Passes.	
APPENDIX III. Electron Density Contours, Vertical Plasma-Drifts and 6300 Å Nightglow Emission Intensities.	

ABSTRACT

This report mainly provides four types of information: 1) Electron density and temperature profiles collected at the Jicamarca Radar Observatory, Lima, Perú, located near the magnetic equator, coincident with twenty near-overhead passes of OGO-VI; 2) Films of Spread-F structure coincident with seven near-overhead passes of OGO-VI; 3) Electron density contours and vertical plasma drifts coincident with five 6300 \AA nightglow emission intensities measured at the Huancayo Observatory; 4) References to papers completed and prepared for publication which are connected with nightglow studies and special events such as a magnetic storm and a solar eclipse.

Introduction

The present report covers work carried at the Jicamarca Radio Observatory of the Instituto Geofísico del Perú (11.95°S 76.87°W , 2° Dip) towards the following objectives, as described in a proposal submitted to the National Aeronautics and Space Administration; 1) Calibration of satellite borne detectors, 2) Supply realistic input data and boundary conditions for theoretical calculations of F-region morphology, and 3) Supply needed boundary values for elucidating the physical processes leading to the nightglow.

This work has been carried in close collaboration with Dr. W. B. Hanson's group at the University of Texas, at Dallas in connection with their satellite borne (OGO-VI) temperature and density probe, and their efforts to mathematically model the dynamics of the equatorial ionospheric phenomena. In addition to the above objectives, concurrent radar and satellite observations of F-region irregularities have been made in an effort to understand the morphology and the cause of the irregularities responsible for Spread-F.

We have performed radar observations and carried on research work in pursuance of the above mentioned objectives as described under the following headlines:

a) Electron Concentration and Temperature and Spread-F Measurement Co-ordinated with OGO-VI Passes

Several kinds of in situ probes are flown in the NASA Satellite Program to obtain global coverage of the ionospheric parameters N_e , T_e , and T_i . The accuracy of the probe measurements can only be obtained if the above parameters are measured by another well established technique.

Such a technique [see Farley, 1969a, b, for its description] is presently used at Jicamarca. We have made simultaneous observations with the radar whenever OGO-VI made a convenient pass over the station.

We have made 25 coincident measurements at dates and times listed in Table I. Concentration and electron temperature measurements have been made during twenty of those days. The results are presented in 40 figures shown in Appendix I. Ion temperatures can be obtained from the electron temperature since, at the equator, both temperatures are approximately equal for height ranges above 300km [McClure, 1969]. Each of the figures shows three vertical profiles, one before and, one after the satellite pass. The consistency between records can be used to indicate the degree of confidence that can be put on the different measurements. More accurate values can be obtained by smoothing in height and time.

The data is currently being compared with OGO-VI concentration and ion temperatures by Dr. Hanson's group at the University of Texas, at Dallas. Preliminary results show good agreement.

Seven of the satellite (OGO-VI) passes occurred at times where Spread-F was present. Whenever irregularities occur, echoes are received several orders of magnitude larger than the incoherent scatter signal received when the medium is in thermodynamic equilibrium. The intensity of these echoes can be used as an indication of the strength of the irregularities that produce them. The irregularities occur in very well defined layers and their height can be accurately determined.

A very useful photographic technique has been developed at the observatory to record the strength of the echoes in a logarithmic way with

the necessary dynamic range. Results are shown in Appendix II. Each frame records the height and strength of the echoes at the time marked along the film. The continuous marks are height marks 100 km apart. The ground pulse is at the bottom of the figure, the echo at 100 km corresponds to the E-region, the rest of the echoes are associated with Spread-F. The length of the white marks is a measure of the intensity of the echoes in db above an arbitrary level (usually noise). The scale is 40 db between two consecutive frames. Two antenna positions are used 6° apart on the E-W plane center around the vertical. They are switched every two frames.

The three days in September were taken using a standard A-scan strip showing only the occurrence and height of the irregularities. The information is being compared with the observations taken by the satellite in collaboration with the University of Texas, at Dallas.

b) Electron Concentration and 6300 \AA Nightglow Measurement

Simultaneous observations of electron density and vertical plasma drifts at Jicamarca and 6300 \AA nightglow emission at Huancayo have been carried out on five nights. The vertical drift has been obtained using a technique recently developed at the observatory [Woodman and Hagfors, 1969]. The electron density data are logarithmic contour plots. The vertical drift velocity is the average value of drifts between 300 and 400 km, except during the presence of coherent echoes (from F-region irregularities) that completely mask the incoherent scatter signal in this altitude range and the average is taken from 400 to 500 km altitude. The dotted positions of the figures indicate the presence of these echoes (equatorial Spread-F). The figures showing the 6300 \AA emission inten-

sities also show the vertical plasma drifts (W_d), the maximum electron concentration (n_m), and the three hours average of K_p . These data are shown in Figures C-1 to C-10. Preliminary analysis and interpretation have been made in a recent comprehensive study of equatorial airglow reported by Lagos and Velásquez [1970]. The information has been made available to the University of Texas, at Dallas for their studies.

c) Special Events

Simultaneous observations of N_e , T_e , and vertical drift were made during the great magnetic storm of March 8, 1970 and, during the September 11, 1969 solar eclipse. The information has been processed and analyzed. The data is presented and interpreted in the following publications:

Woodman, R. F., "Jicamarca incoherent scatter observations during the March 1970 storm", in WDC-A Upper Atmosphere Geophysics, Boulder, Colorado. Data on Solar Geophysical Activity Associated with the Major Geomagnetic Storm of March 8, 1970, Rept. UAG-12, April 1971, 3 Parts, pp. 194-199.

Sterling, D. L., W. B. Hanson, and R. F. Woodman, "Synthesis of equatorial data from Jicamarca, Peru, during the September 11, 1969 eclipse"; submitted for publication to Radio Science.

Woodman, R. F., D. L. Sterling, and W. B. Hanson, "Synthesis of Jicamarca data during the great storm of March 8, 1970"; to be submitted to Radio Science.

The last two publications include synthesis of the data obtained using the mathematical model developed by Hanson and Sterling of the University of Texas, at Dallas. The agreement is very good, showing that

there is now a very good understanding of the physical and chemical processes of the equatorial ionosphere. There is only one important parameter that has not been measured yet, and that is needed for unambiguously modeling the equatorial ionosphere: the North South component of the ion velocity due to the drag caused by the NS component of the neutral wind.

Acknowledgement. The authors wish to thank the Jicamarca Staff for their technical assistance.

REFERENCES

- Farley, D. T., "Incoherent scatter correlation function measurements", Radio Sci., 4, 935-953 (Oct. 1969)
- Farley, D. T., "Incoherent scatter power measurements; a comparison of various techniques", Radio Sci., 4, 139-142 (Feb. 1969)
- McClure, J. P., "Diurnal variation of neutral charged particle temperatures in the equatorial F region", J. Geophys. Res., 279-291 (Jan. 1, 1969).
- Woodman, R. F. and T. Hagfors, "Methods for the measurements of vertical ionospheric motions near the magnetic equator by incoherent scattering", J. Geophys. Res., 74, 1205-1212 (March 1, 1969)
- Lagos, C. P. and A. Velásquez, "Studies of equatorial airglow". Final technical report. Instituto Geofísico del Perú, 1970.

TABLE I

OGO-VI Passes

DATE	LOCAL TIME	HEIGHT	REMARKS
Oct. 31, 1969	1127	943 km	N _e , T _e
Oct. 31, 1969	2349	635 km	N _e , T _e
Nov. 12, 1969	1110	467 km	N _e , T _e
Nov. 15, 1969	2206	433 km	N _e , T _e
Mar. 7, 1970	0637	479 km	N _e , T _e
Mar. 7, 1970	0816	453 km	N _e , T _e
Mar. 8, 1970	0727	467 km	N _e , T _e
Mar. 8, 1970	1958	-----	N _e , T _e
Aug. 6, 1970	1156	625 km	N _e , T _e
Aug. 8, 1970	1148	639 km	N _e , T _e
Aug. 17, 1970	2252	539 km	N _e , T _e
Aug. 30, 1970	2109	421 km	N _e , T _e
Sept. 1, 1970	0831	1038 km	N _e , T _e
Sept. 3, 1970	0822	1021 km	N _e , T _e
Sept. 10, 1970	1928	553 km	Film
Sept. 12, 1970	1919	506 km	N _e , T _e Film
Sept. 14, 1970	1909	459 km	N _e , T _e Film
Sept. 29, 1970	1711	676 km	N _e , T _e
Oct. 1, 1970	1901	708 km	N _e , T _e
Oct. 30, 1970	0113	509 km	N _e , T _e
Nov. 1, 1970	0101	605 km	N _e , T _e
Nov. 19, 1970	2217	488 km	Film
Nov. 21, 1970	2204	514 km	Film
Nov. 23, 1970	2150	517 km	Film
Nov. 25, 1970	2137	547 km	Film

APPENDIX I

Figure Captions.

Fig. A 1a) to A 20a Electron density profiles for the times (75°W) and date indicated in the figure. There was a near overhead OGO-VI pass within the period at a time and height shown in Table I of the main text.

Fig. A1b) to A 10b Same as above, but the electron temperature profile is shown.

APPENDIX II

Figure Captions

Fig. B1 to B4 Photographic prints of a film strip showing the structure, height, thickness, and strength of F-region irregularities responsible for Spread-F and satellite scintillations. The film is centered around the time of a near overhead satellite pass shown in Table I. The vertical scale is 100 km in between continuous lines. The longest of the traces at the bottom correspond to the transmitter pulse interference. The next higher (100 km) traces correspond to the electrojet. All higher traces are due to the presence of F-region irregularities. The length of the trace is a measure of the strength of the echoes with a scale of 40 db between frames.

Fig. B5 to B7 These show similar information as in B1 to B4, but there is no quantitative indication of the strength of the echo. A wider transmitter pulse was used in these cases. The two lines on the top of the figure on September 10, correspond to the next transmitter pulse.

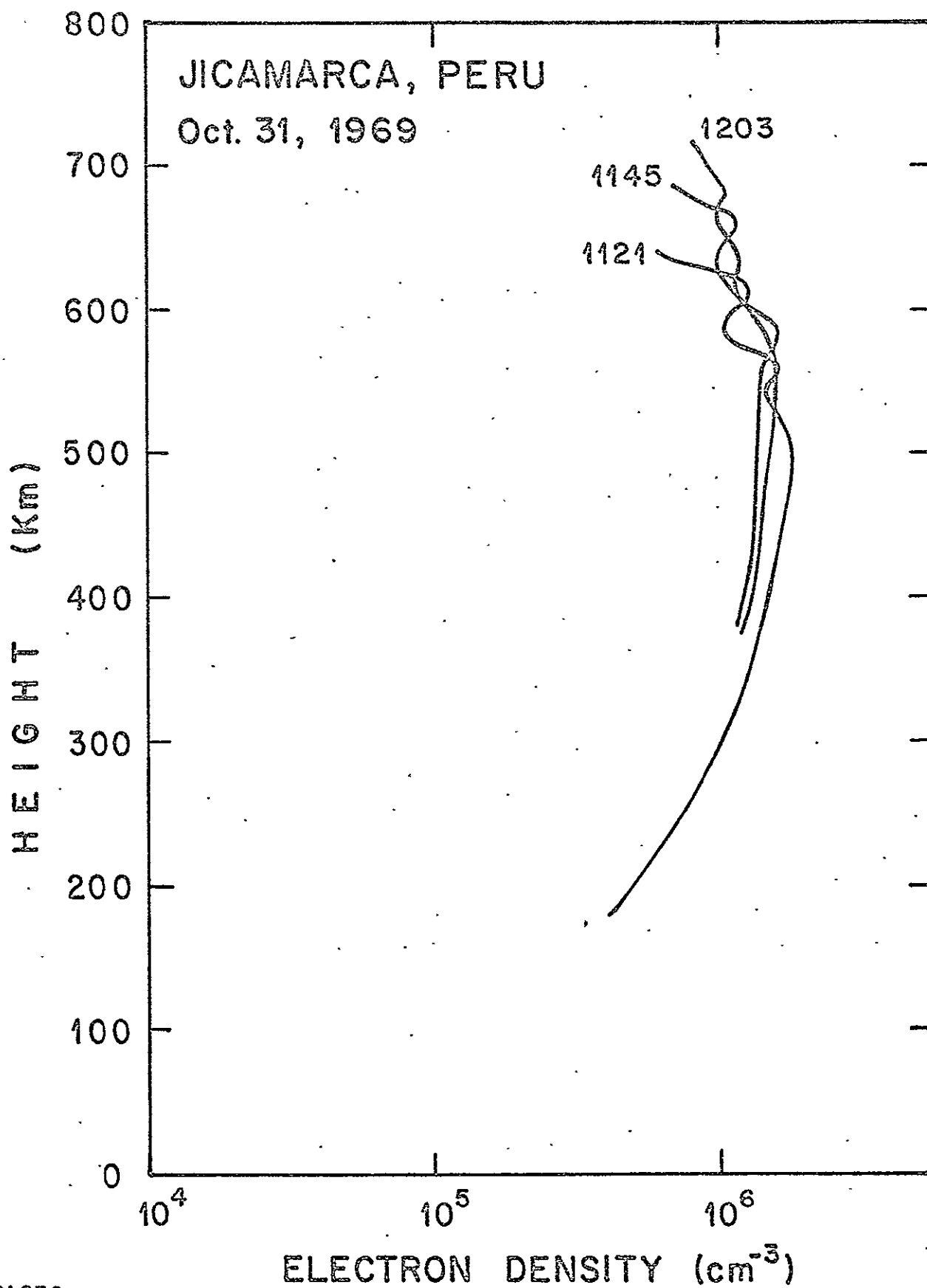
APPENDIX III

Figure Captions.

- Fig. C 1a) to C 5a Electron density contour plots in a base ten logarithmic scale and the corresponding vertical drift velocity.
- Fig. C 1b) to C 5b 6300 Å nightglow emission intensity corresponding to the densities in Figures C 1a) to C 5a. The vertical velocity W_d , maximum density, N_m , and height of the maximum, h_m , is also depicted.

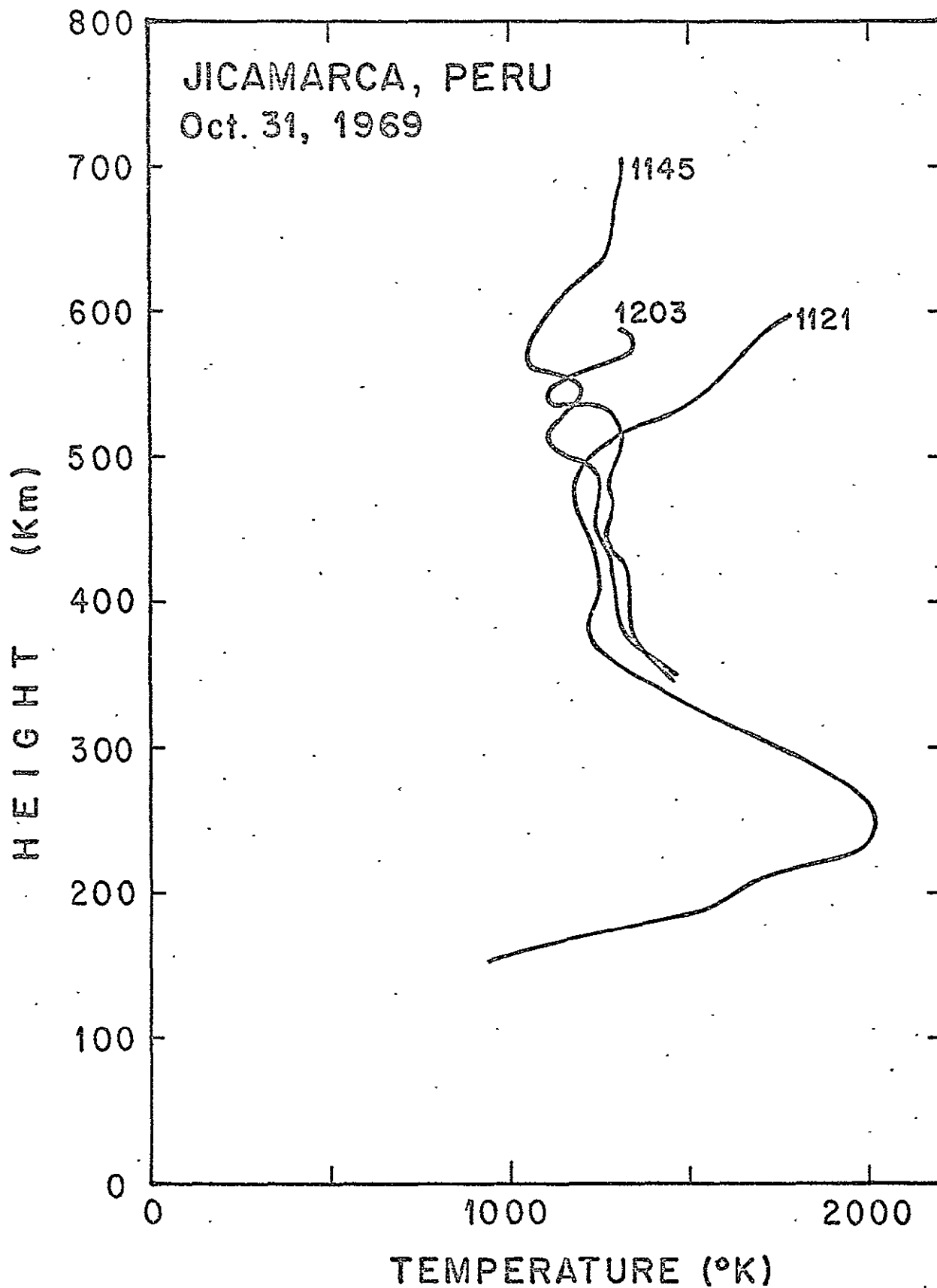
APPENDIX I

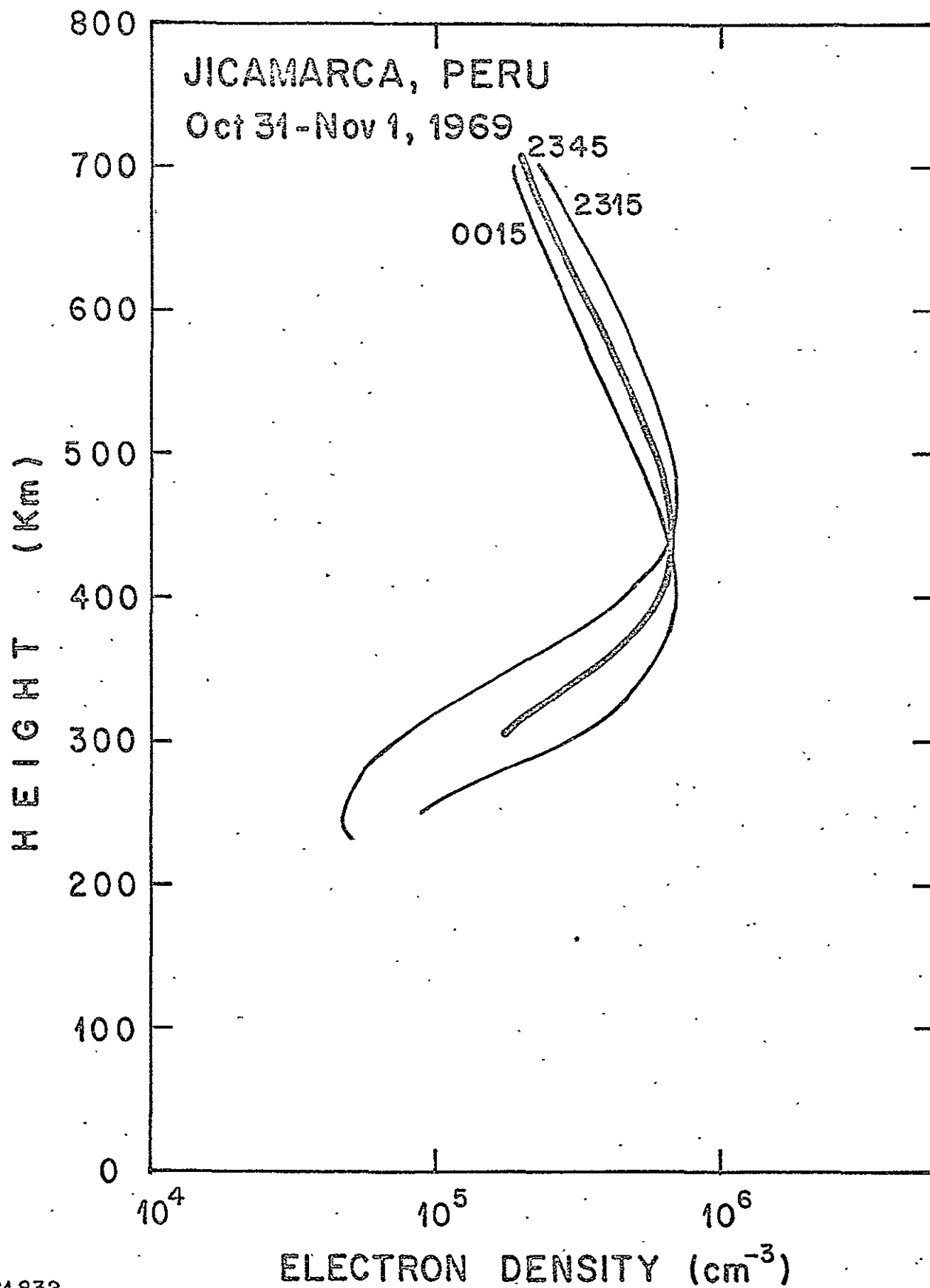
ALTITUDE PROFILES OF N_e AND T_e COINCIDENT WITH OGO VI PASSES



N°1830
JICAM-22/Jun/71
P.L./aloht.

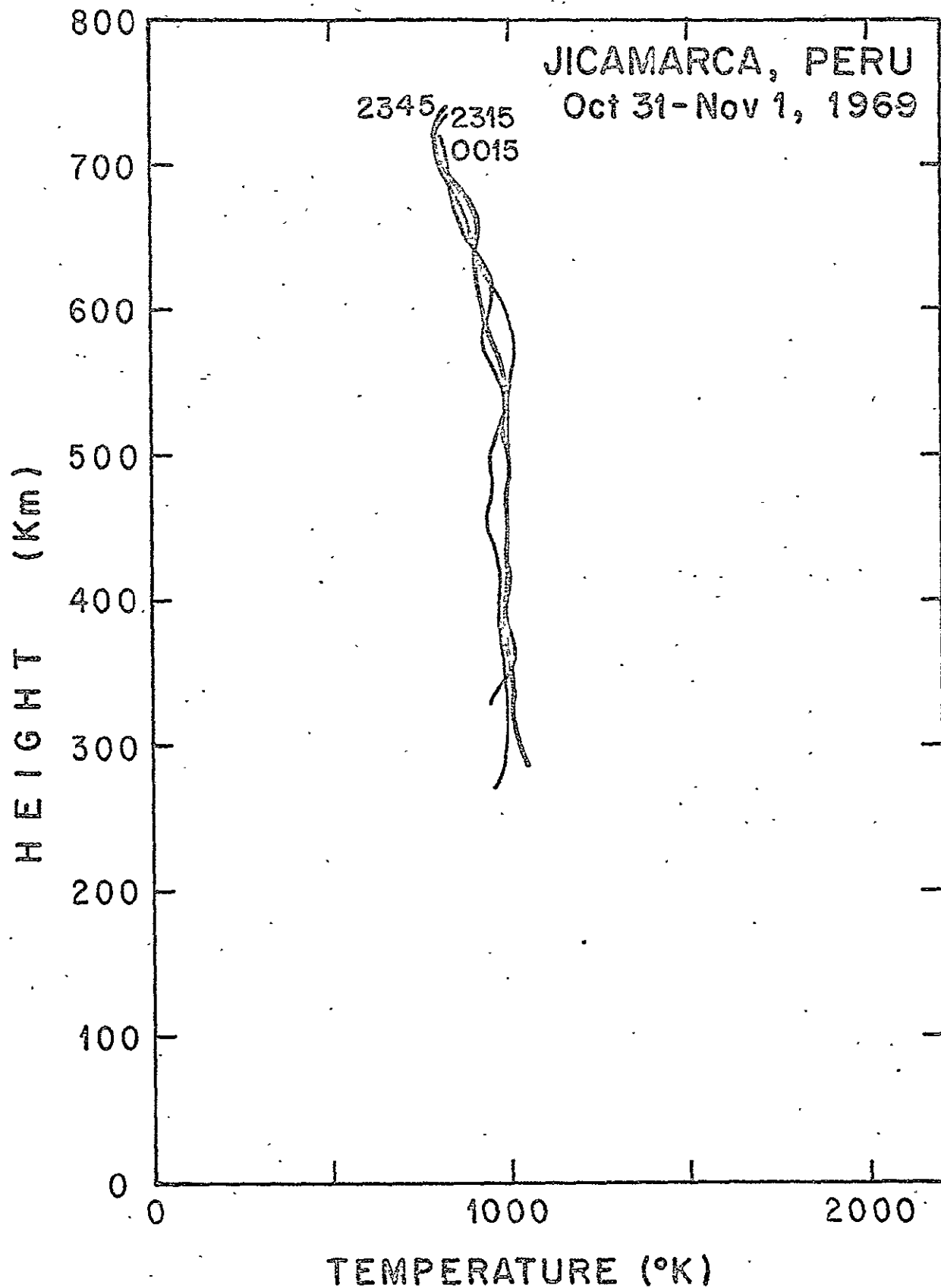
Fig 1a





N°1832
JICAM-23/Jun/71
P.L./aloht.

Fig 2a:



Nº 1831
JICAM: 23/Jun/71
P.L./alohf.

Fig 2b

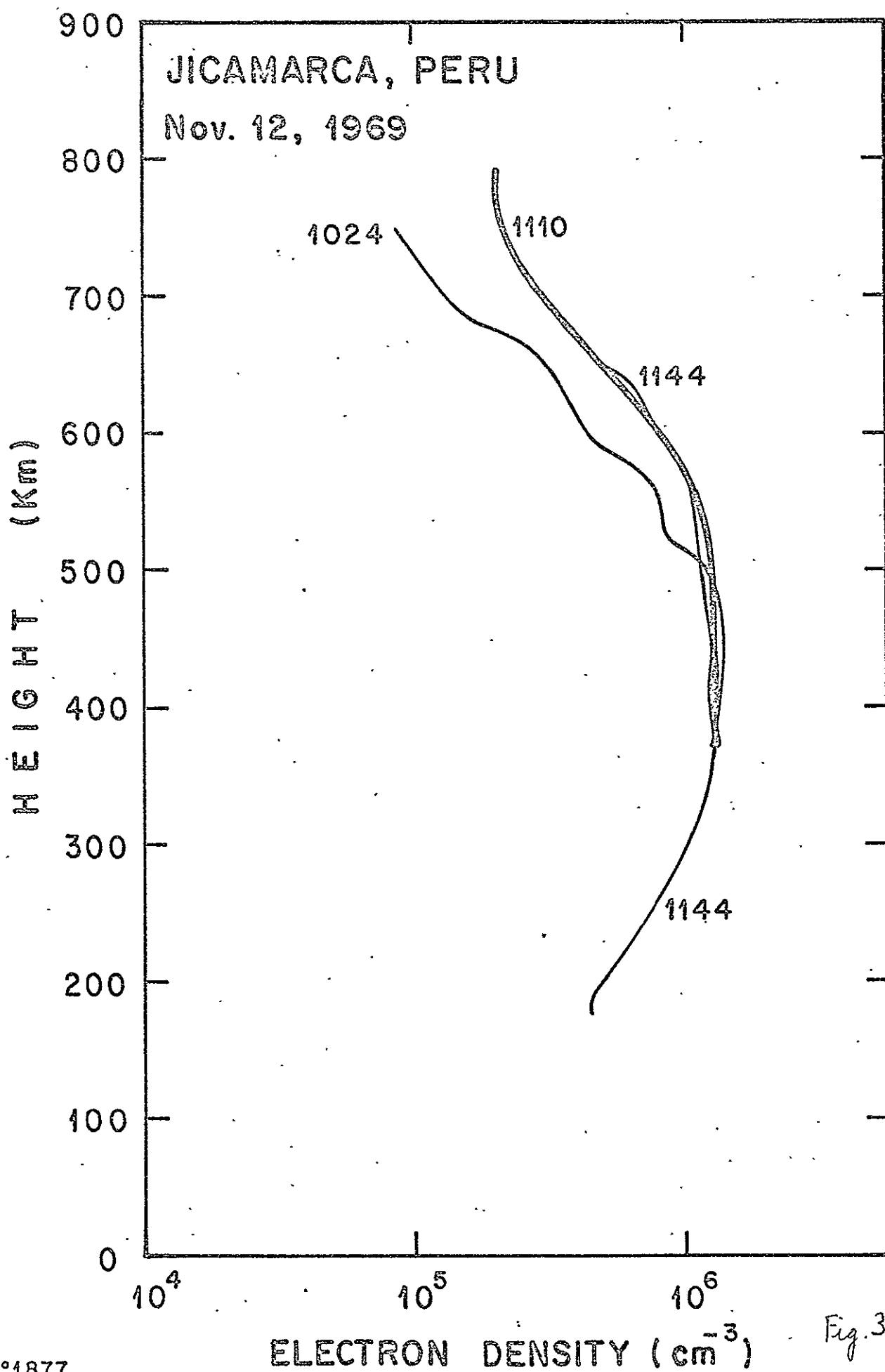
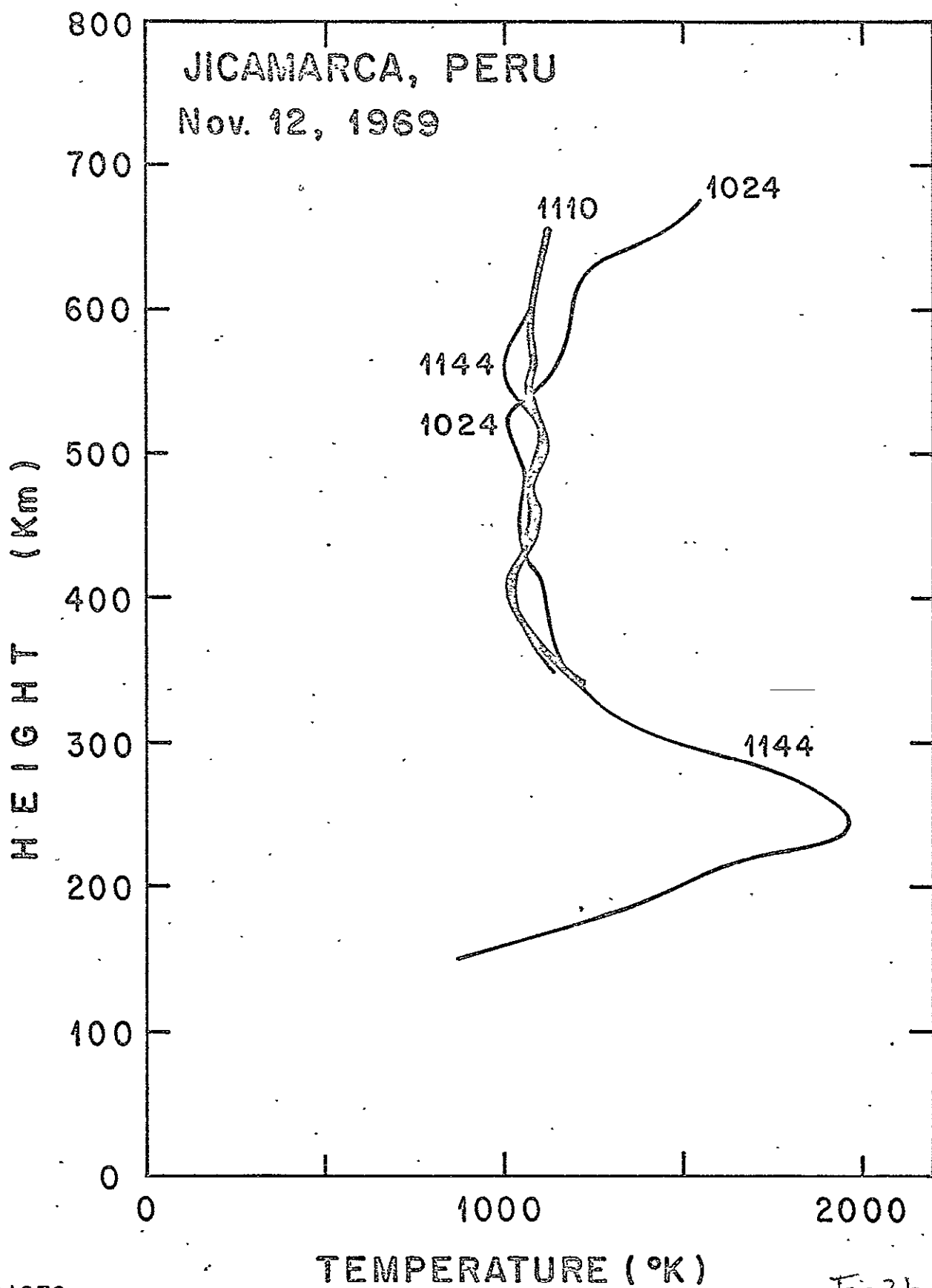
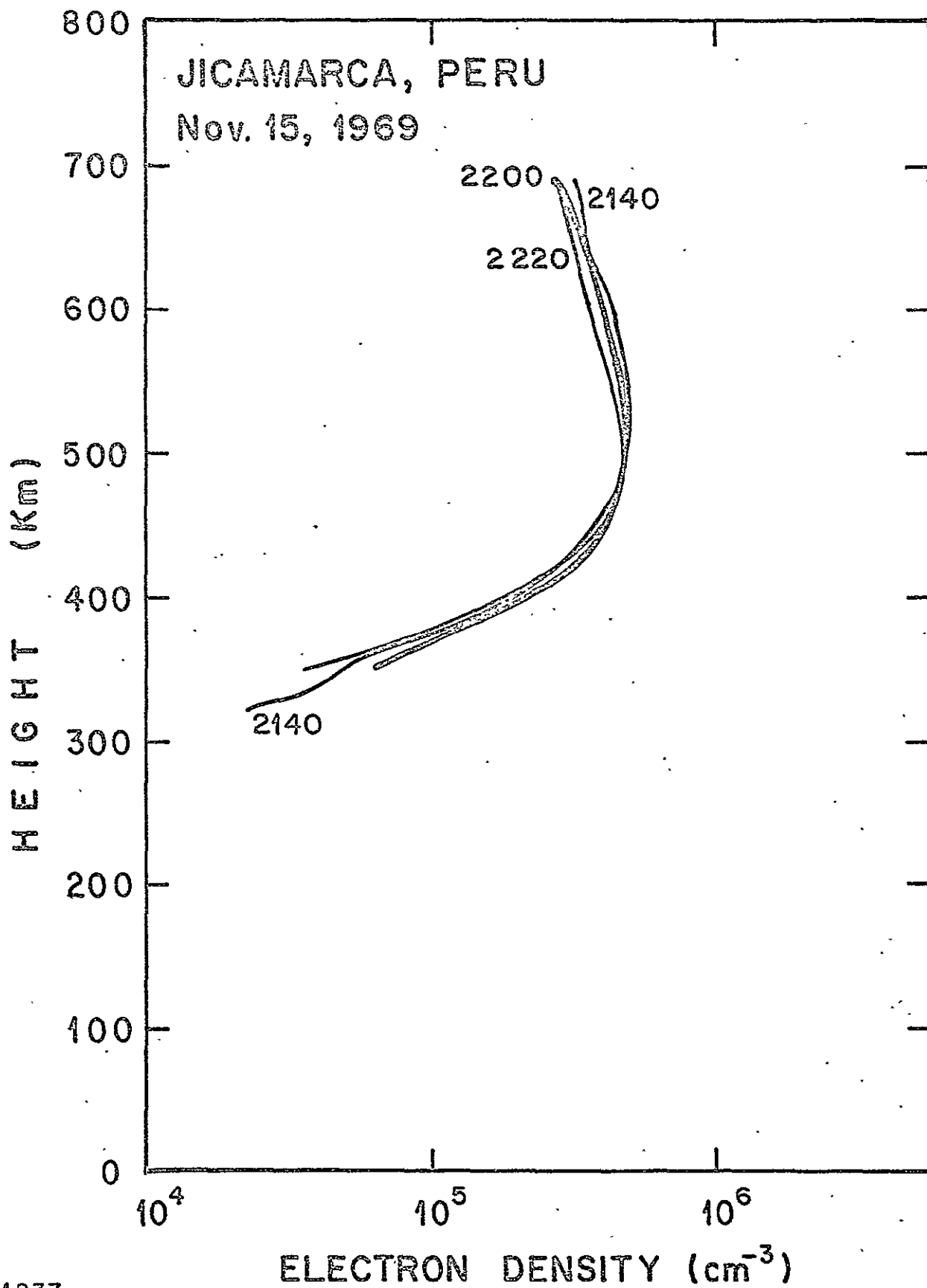
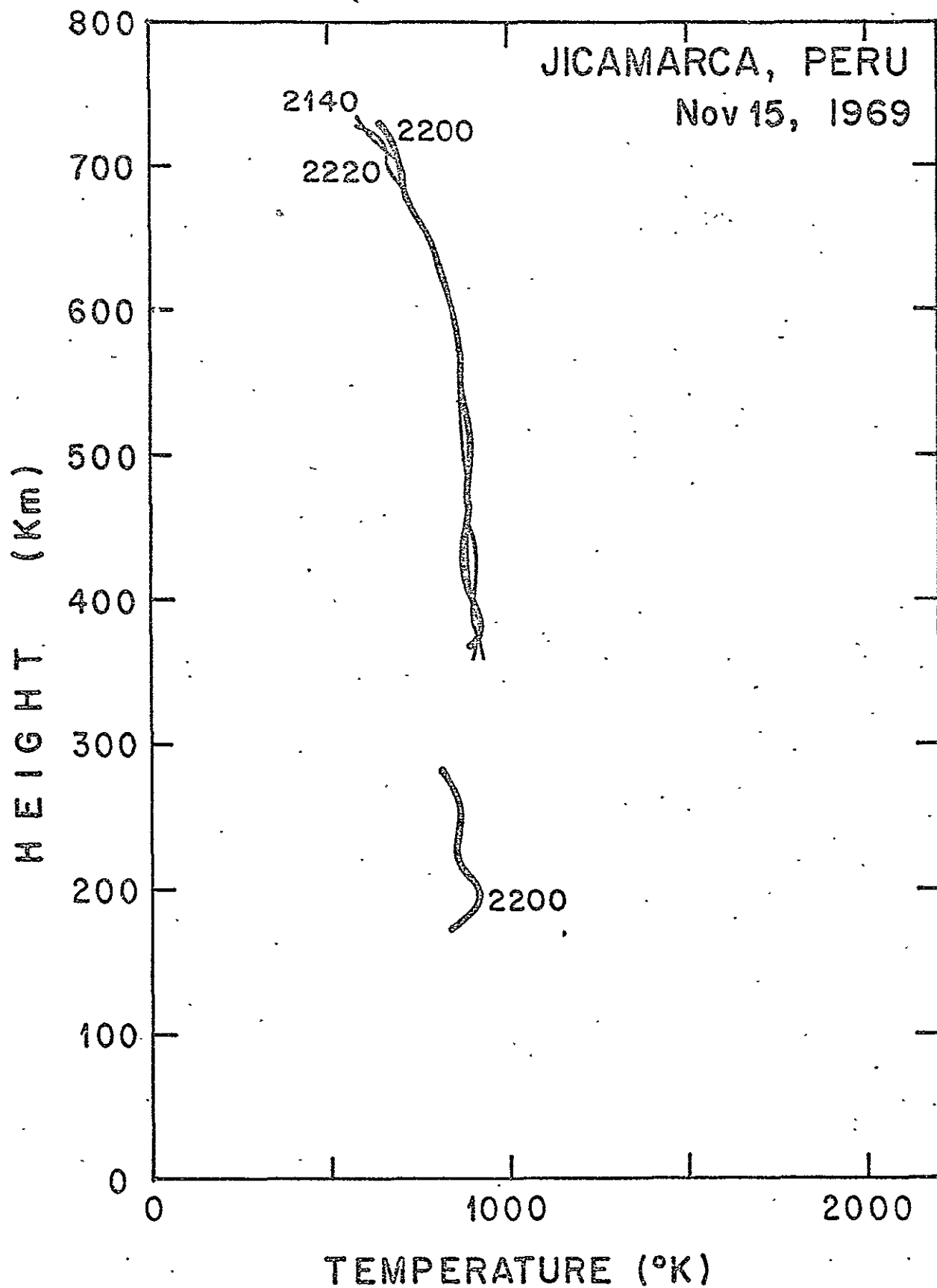


Fig. 3a

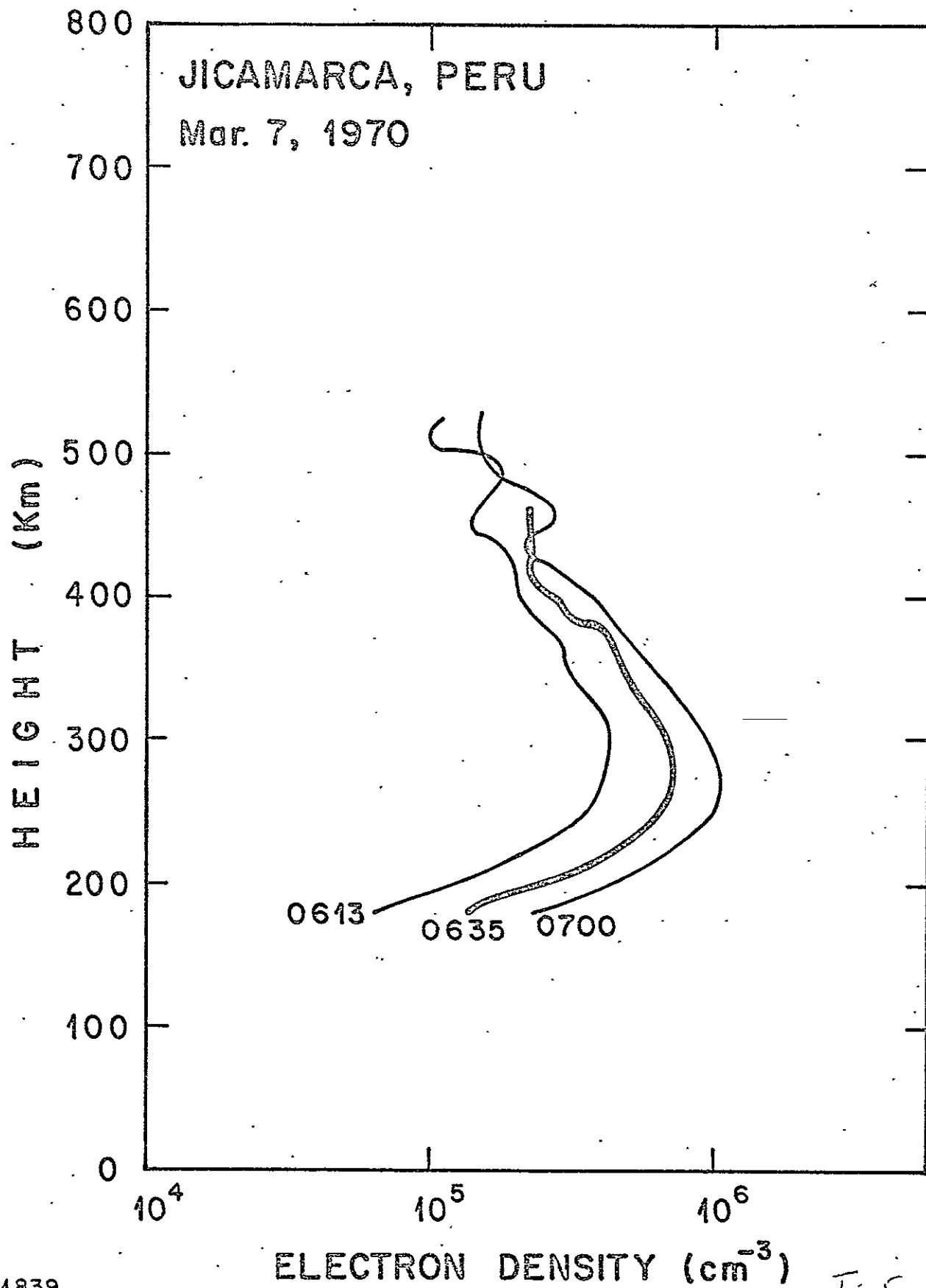






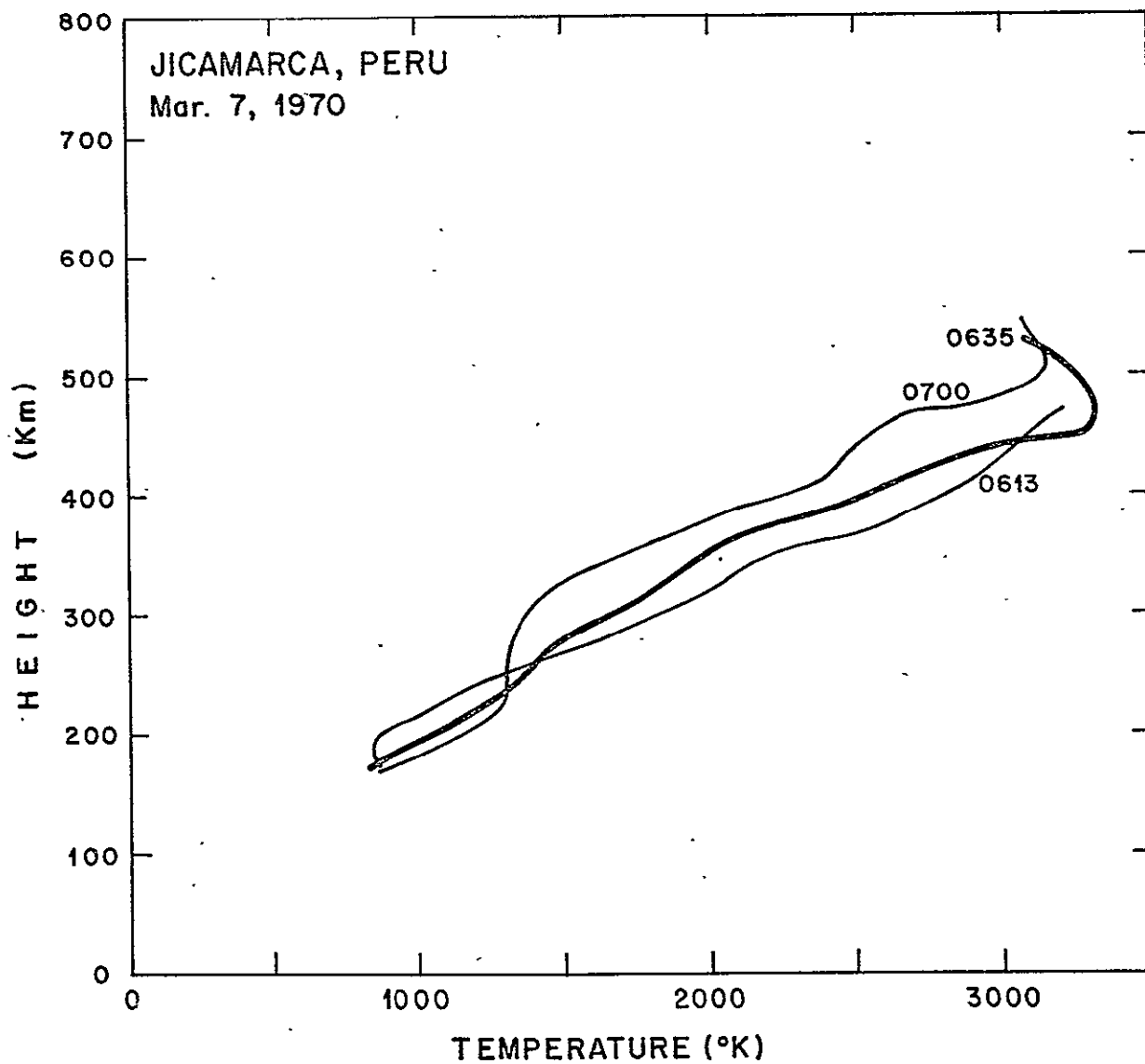
N°1836
JICAM-25/Jun/71
P.L./aloht.

Fig 4b



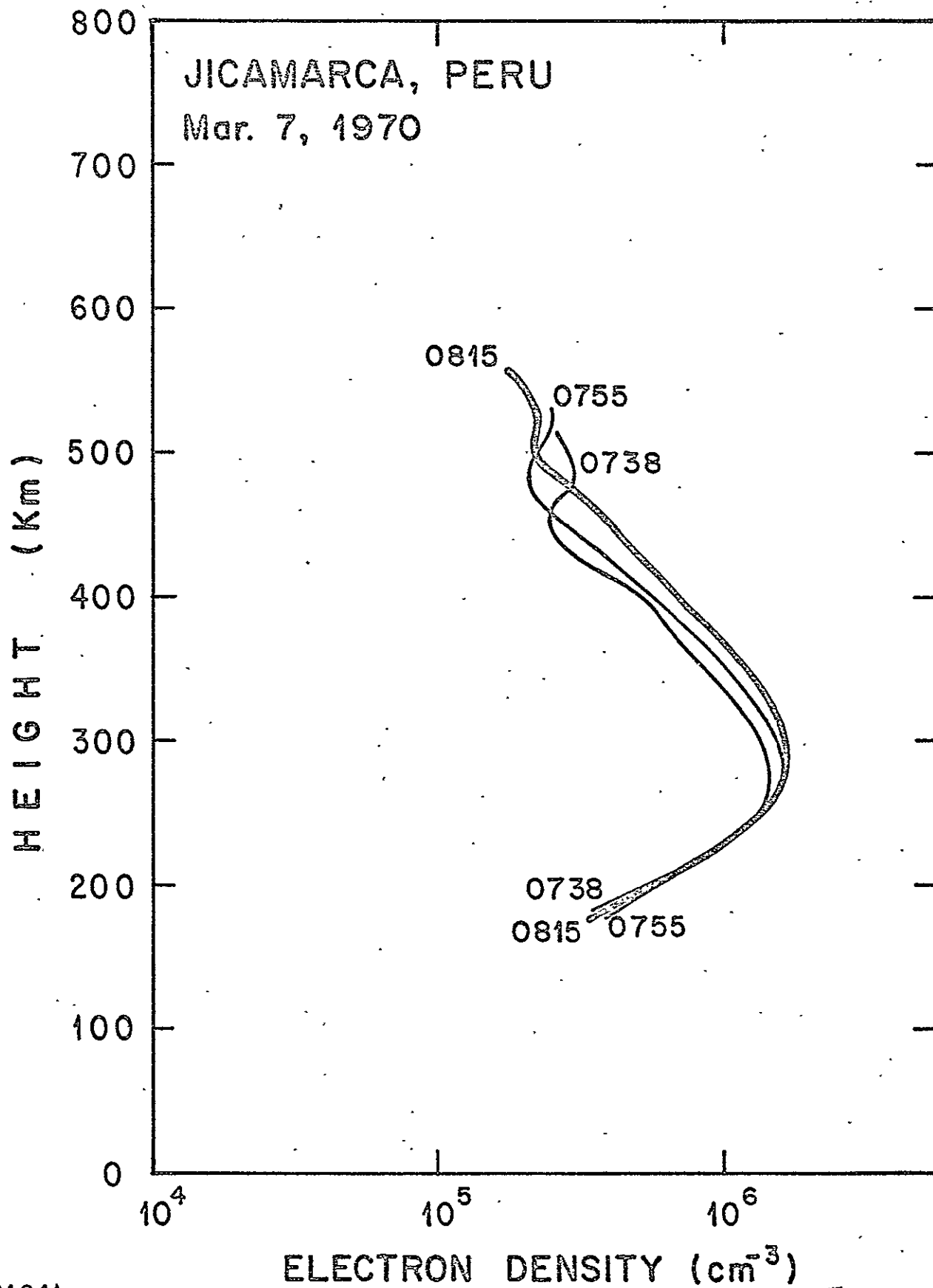
N°1839
JICAM-25/Jun/71
P.L./aloht.

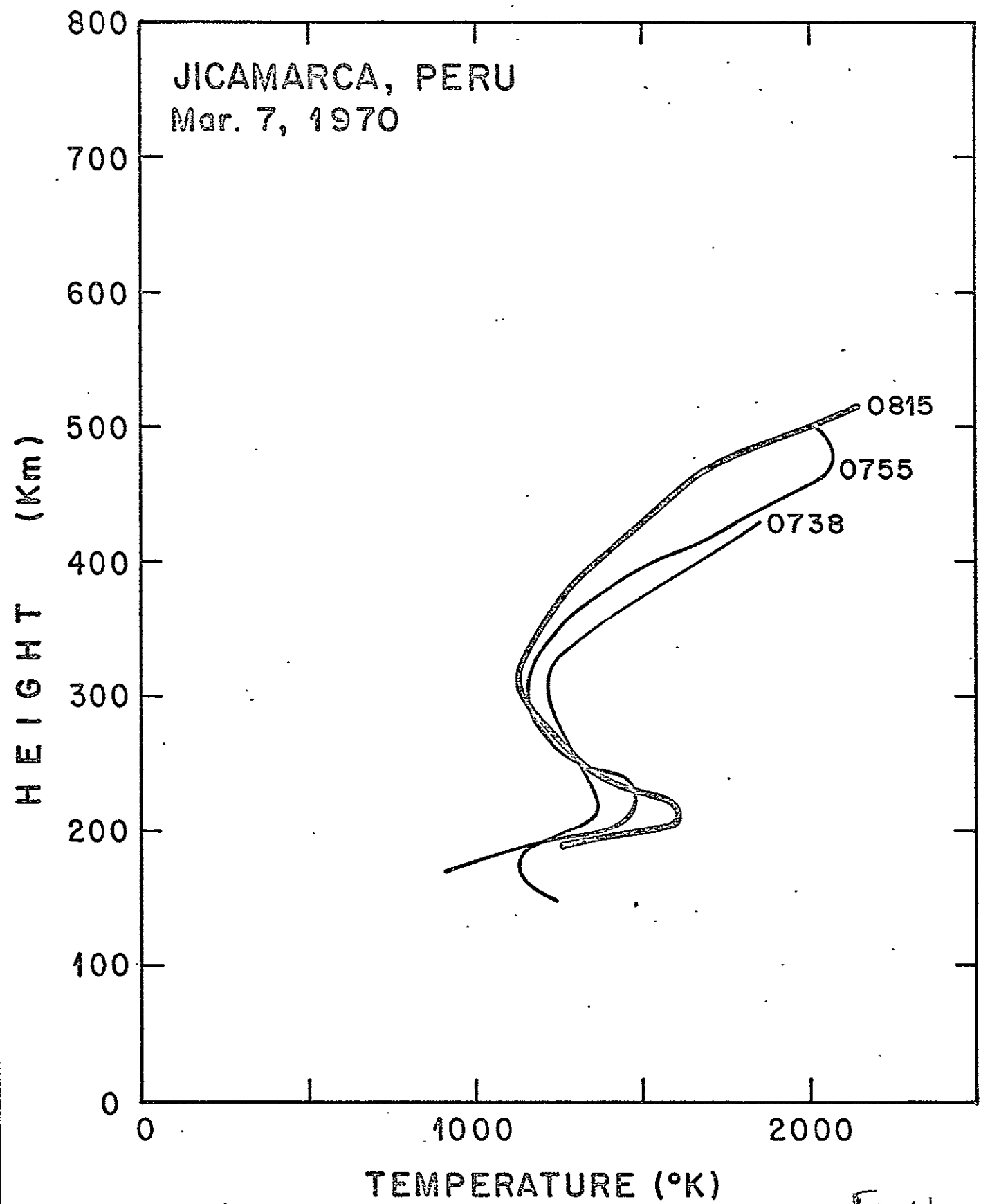
Fig 5a



N°1838
JICAM.-25/Jun/71
P.L./aloh.

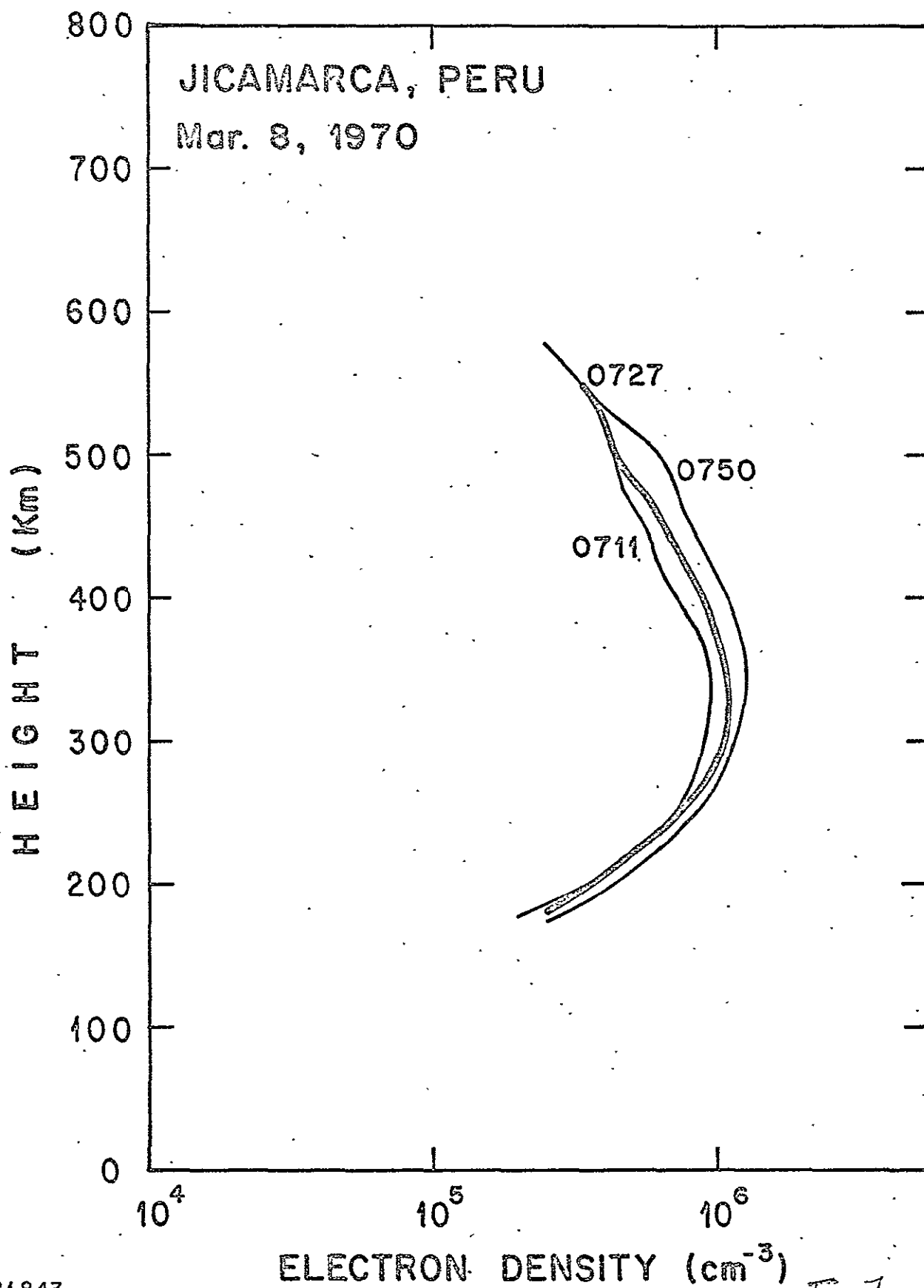
Fig. 5b

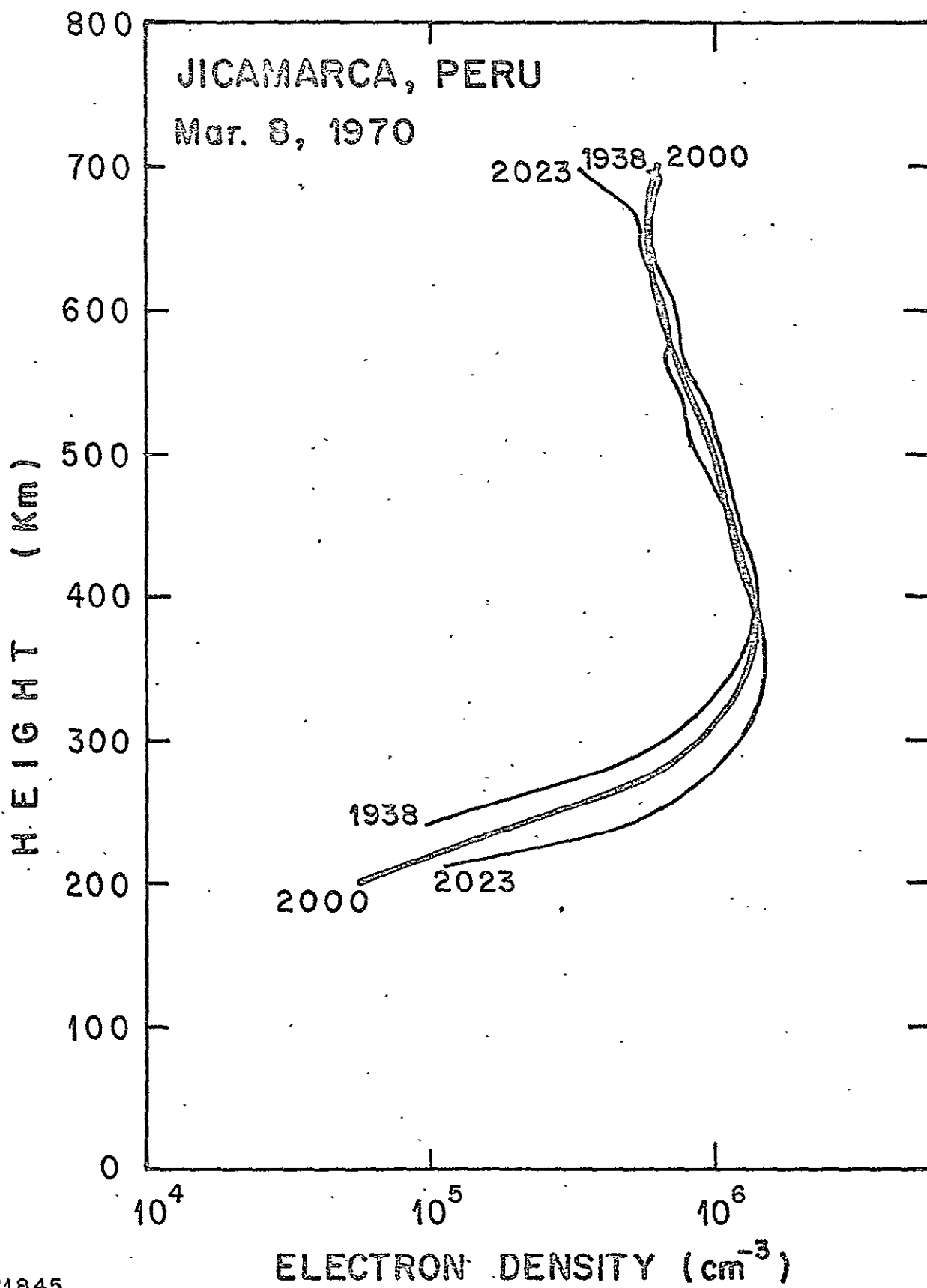




1840
CAM-28/Jun/71
L./aloh.

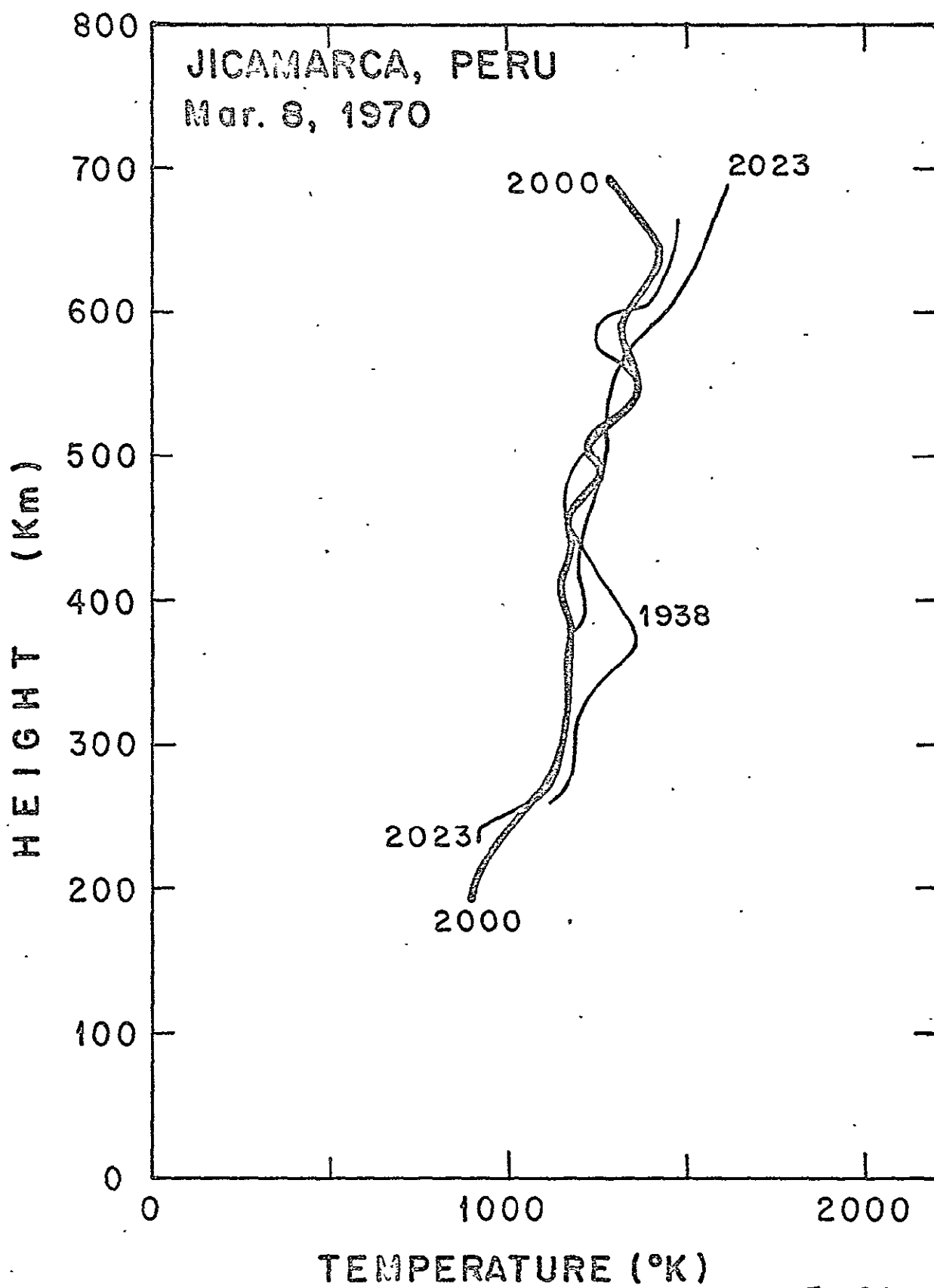
Fig 6b

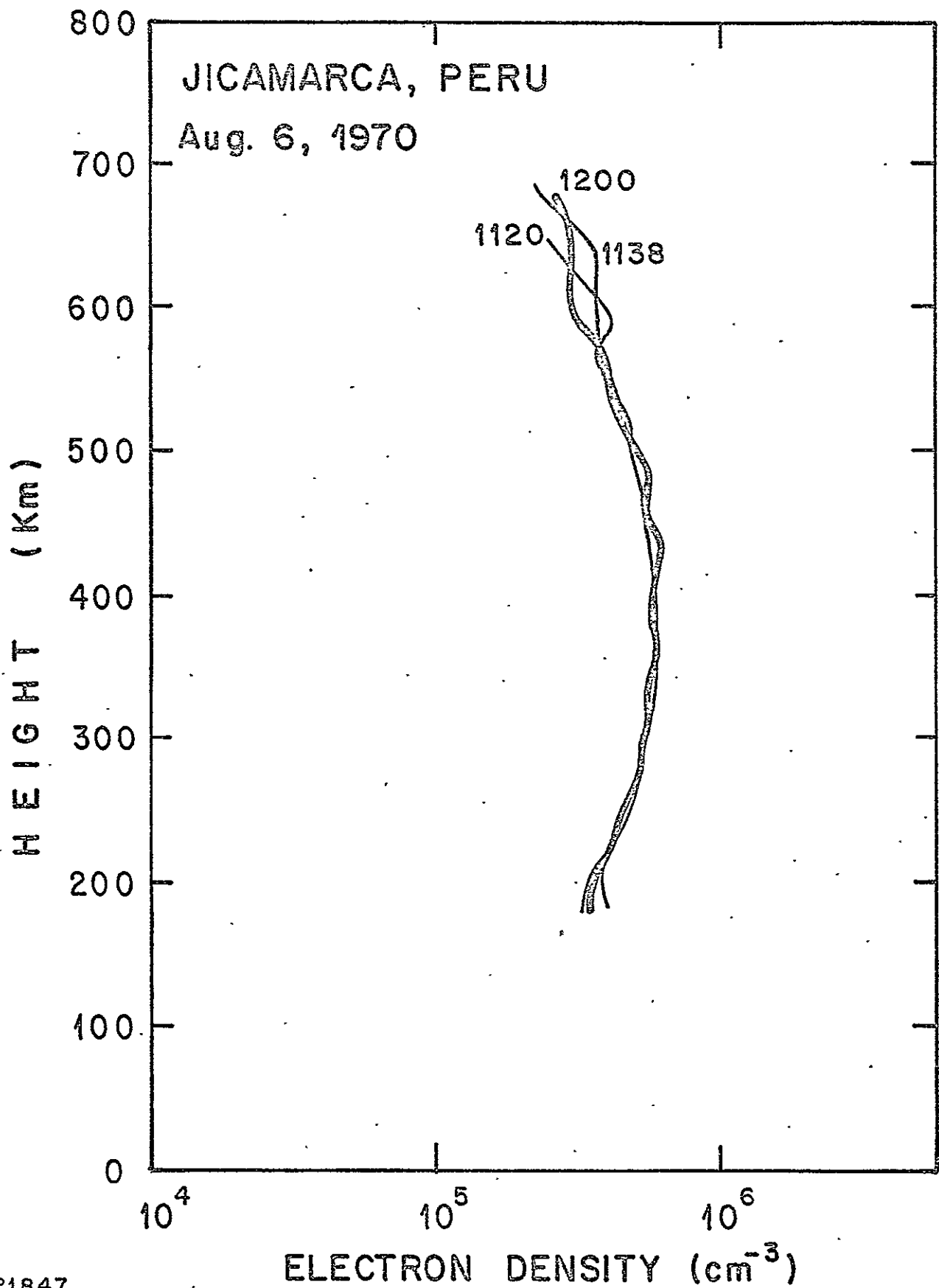




Nº1845
JICAM.-1º/Jul. /71
P.L./aloht.

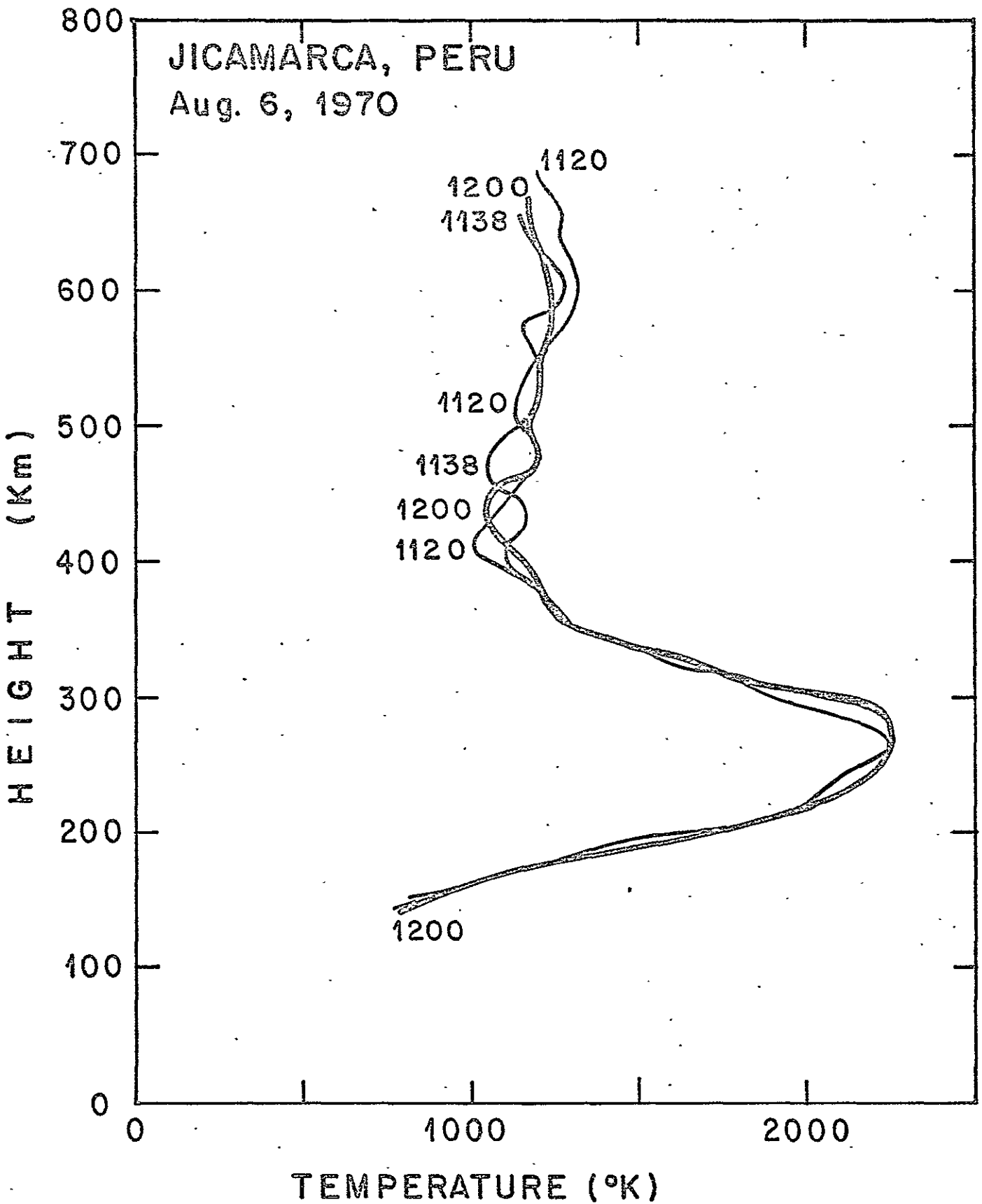
Fig 8a





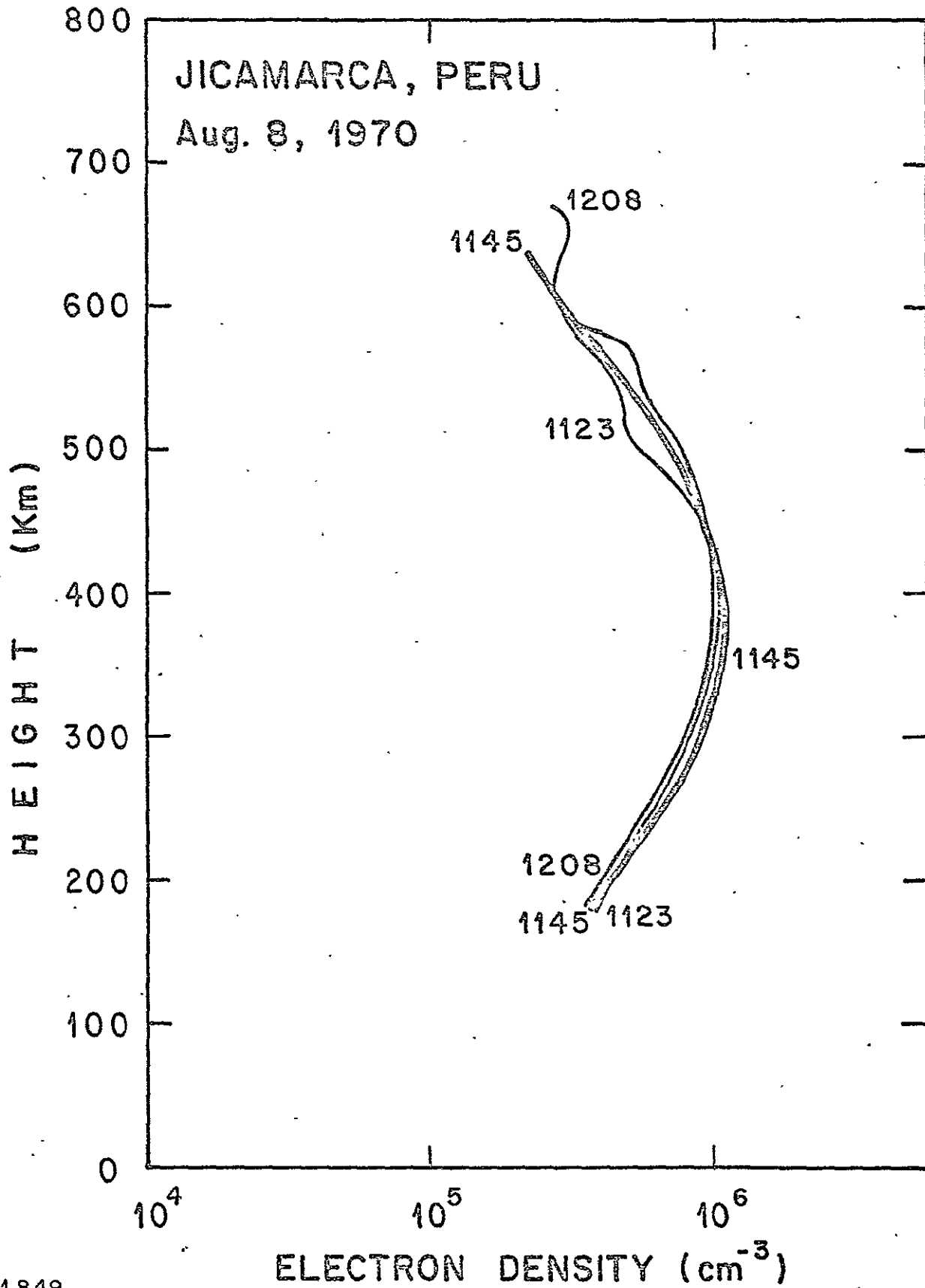
N°1847
JICAM-1°/Jul./71
P.L./alohi.

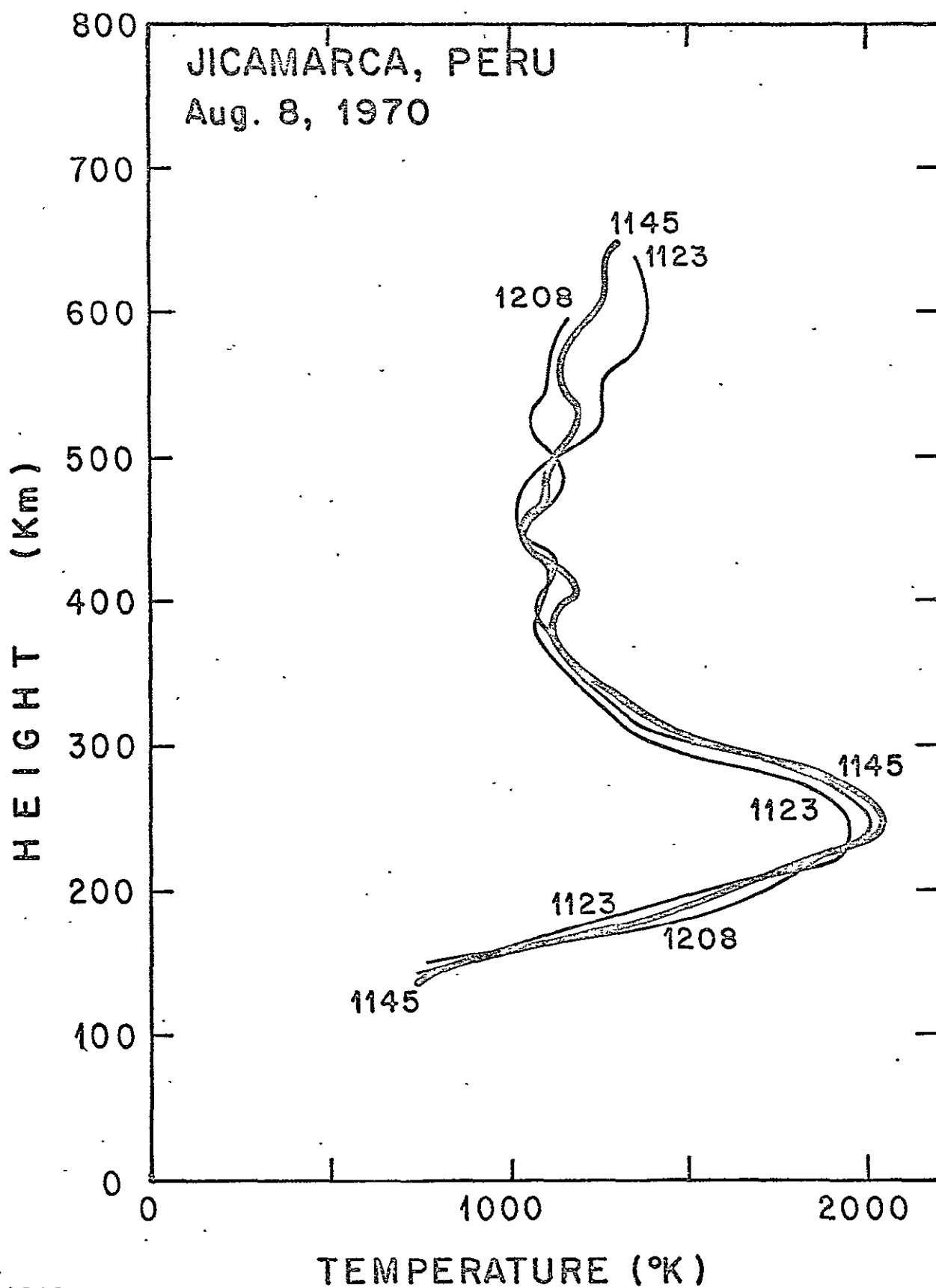
Fig 9a

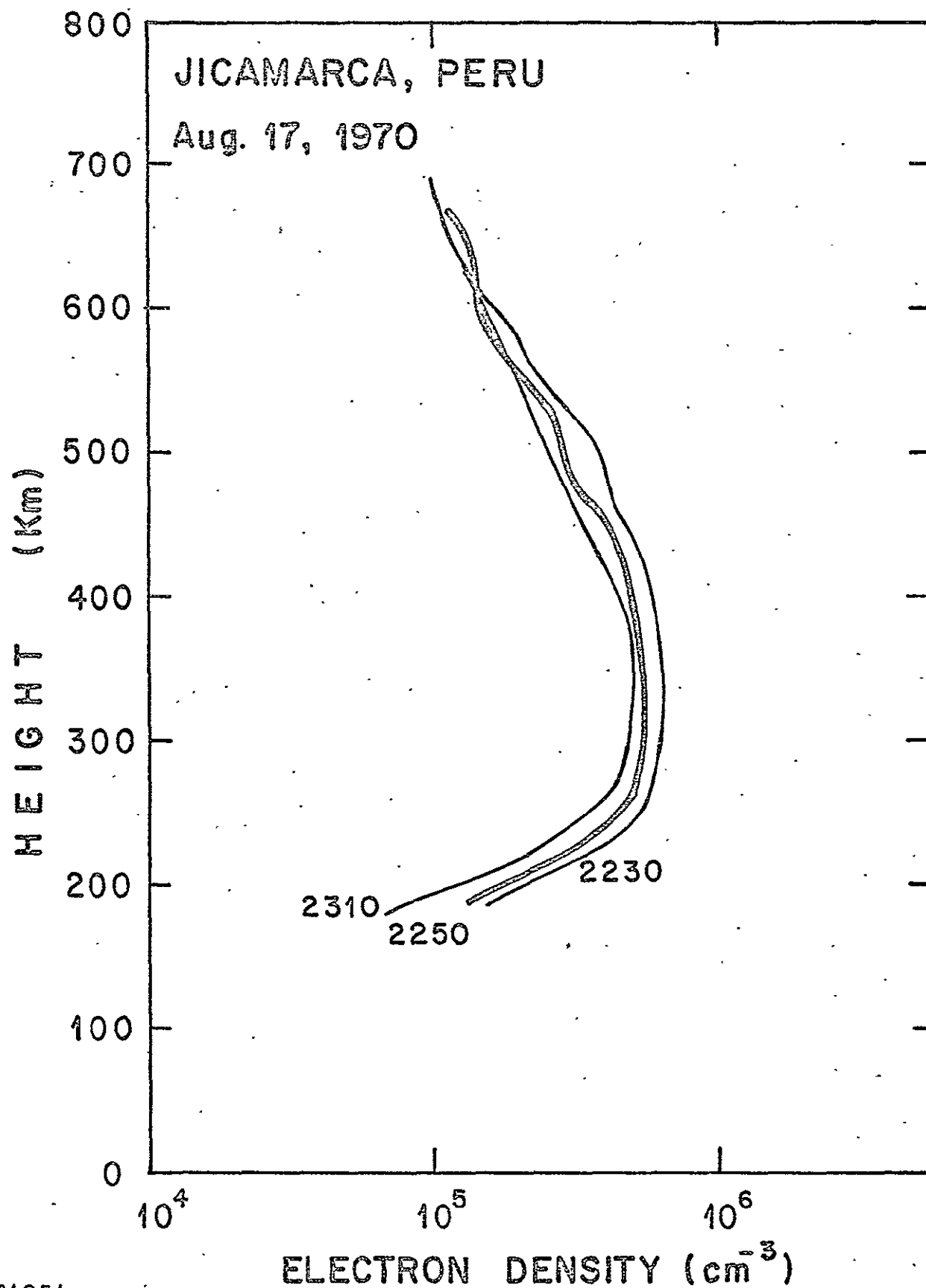


1846
JICAM-1°/Jul/74
L./alght.

Fig 9b

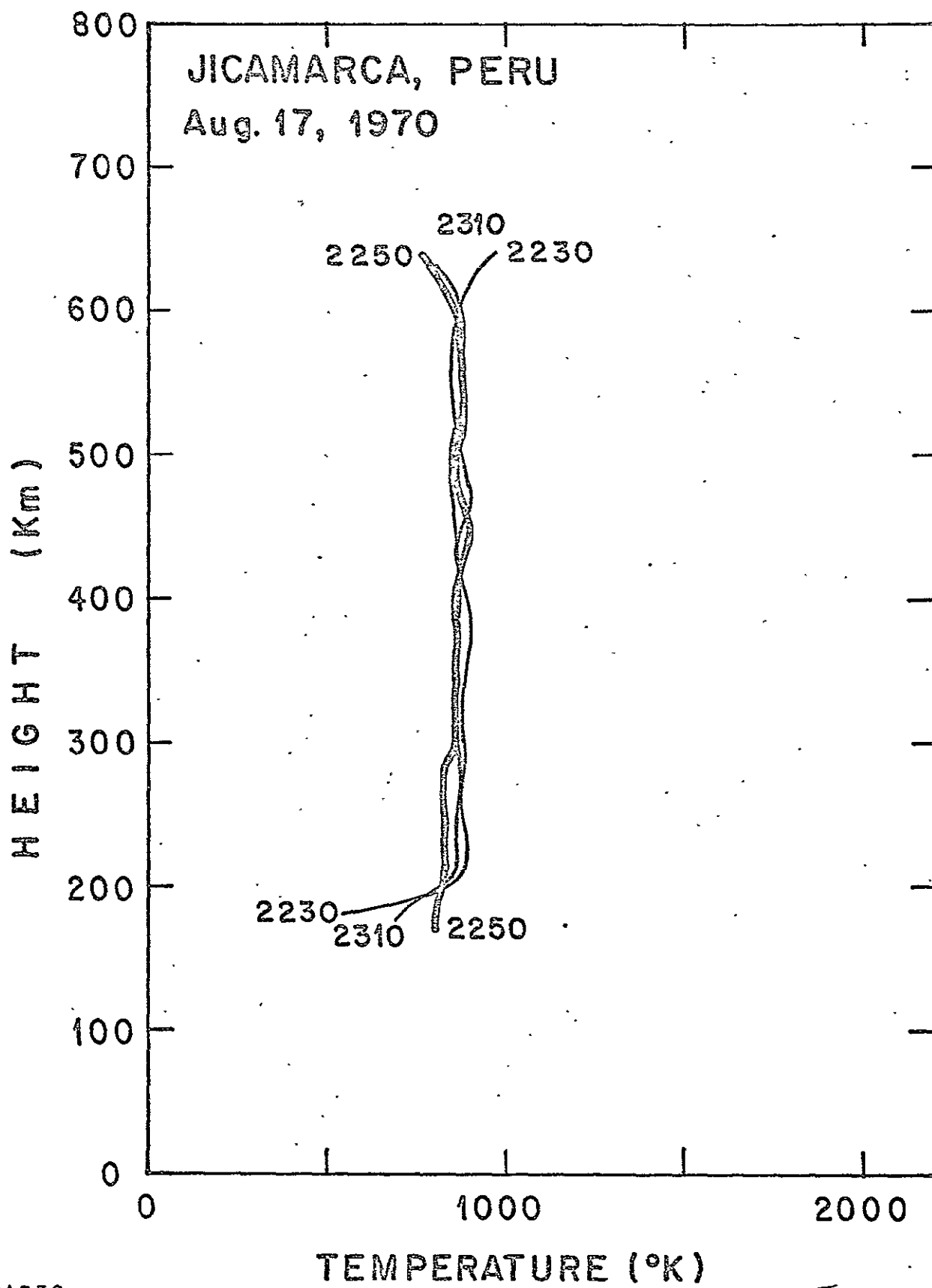






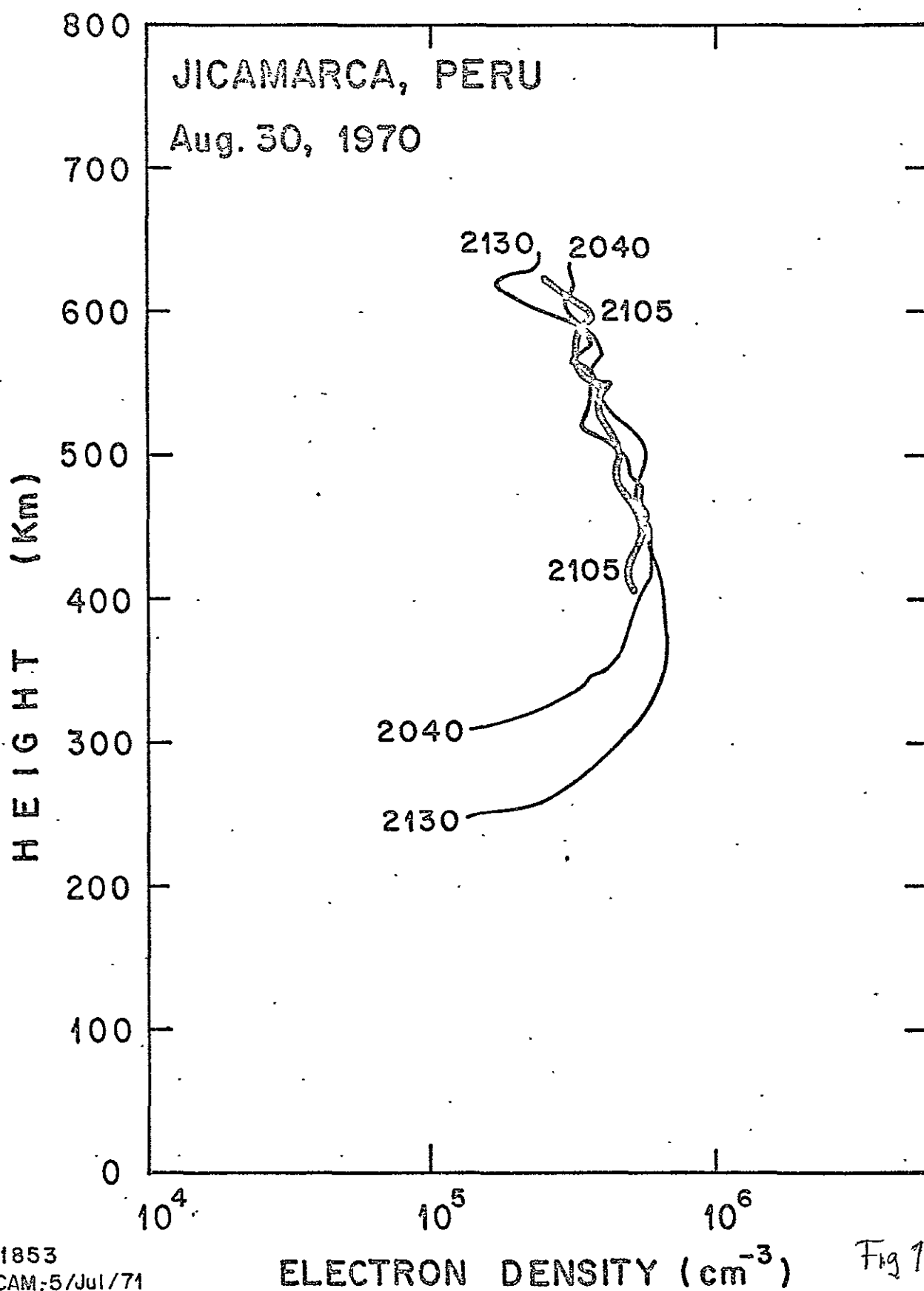
N°1854
JICAM-2/Jul/74
P.L / aloht.

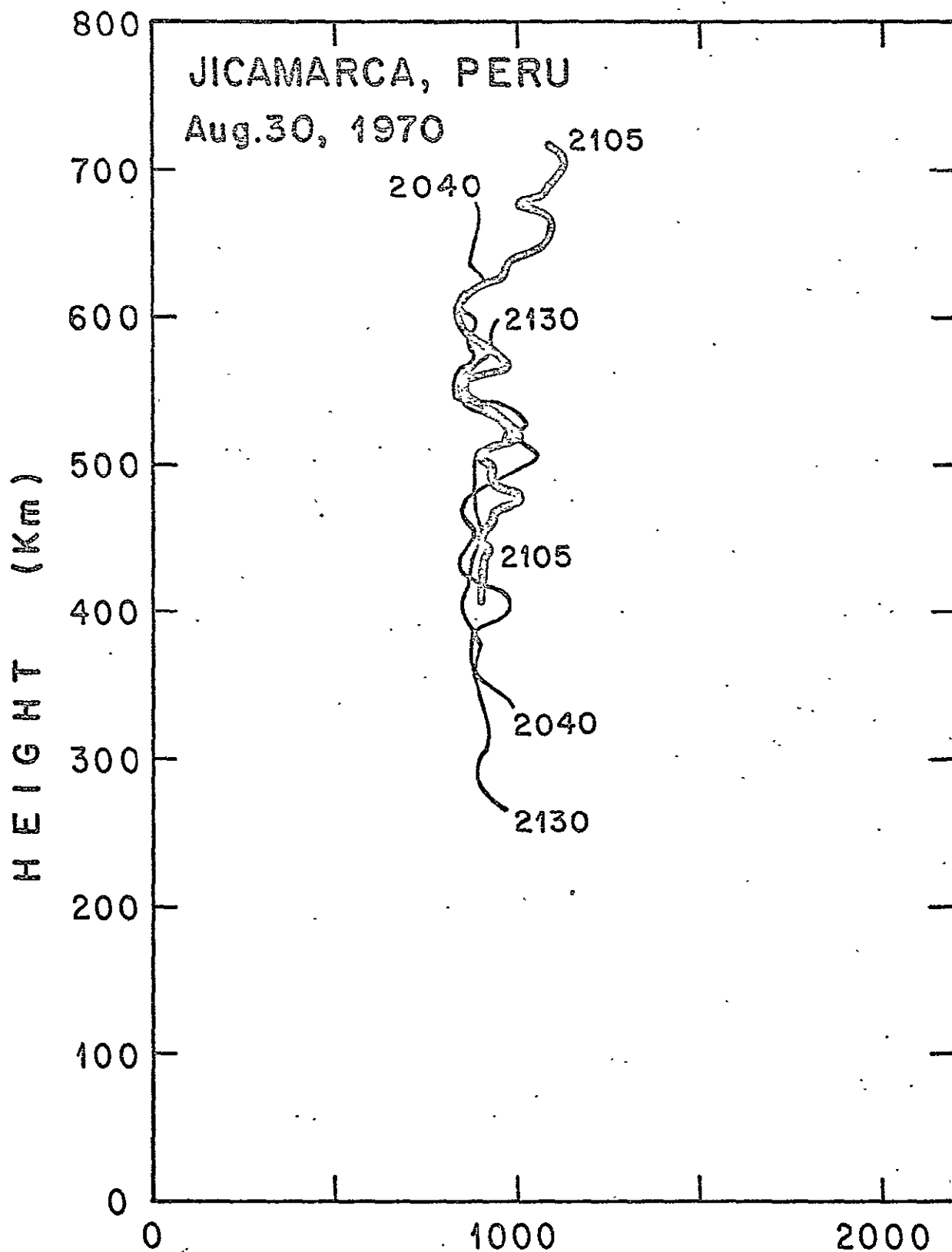
Fig 11a

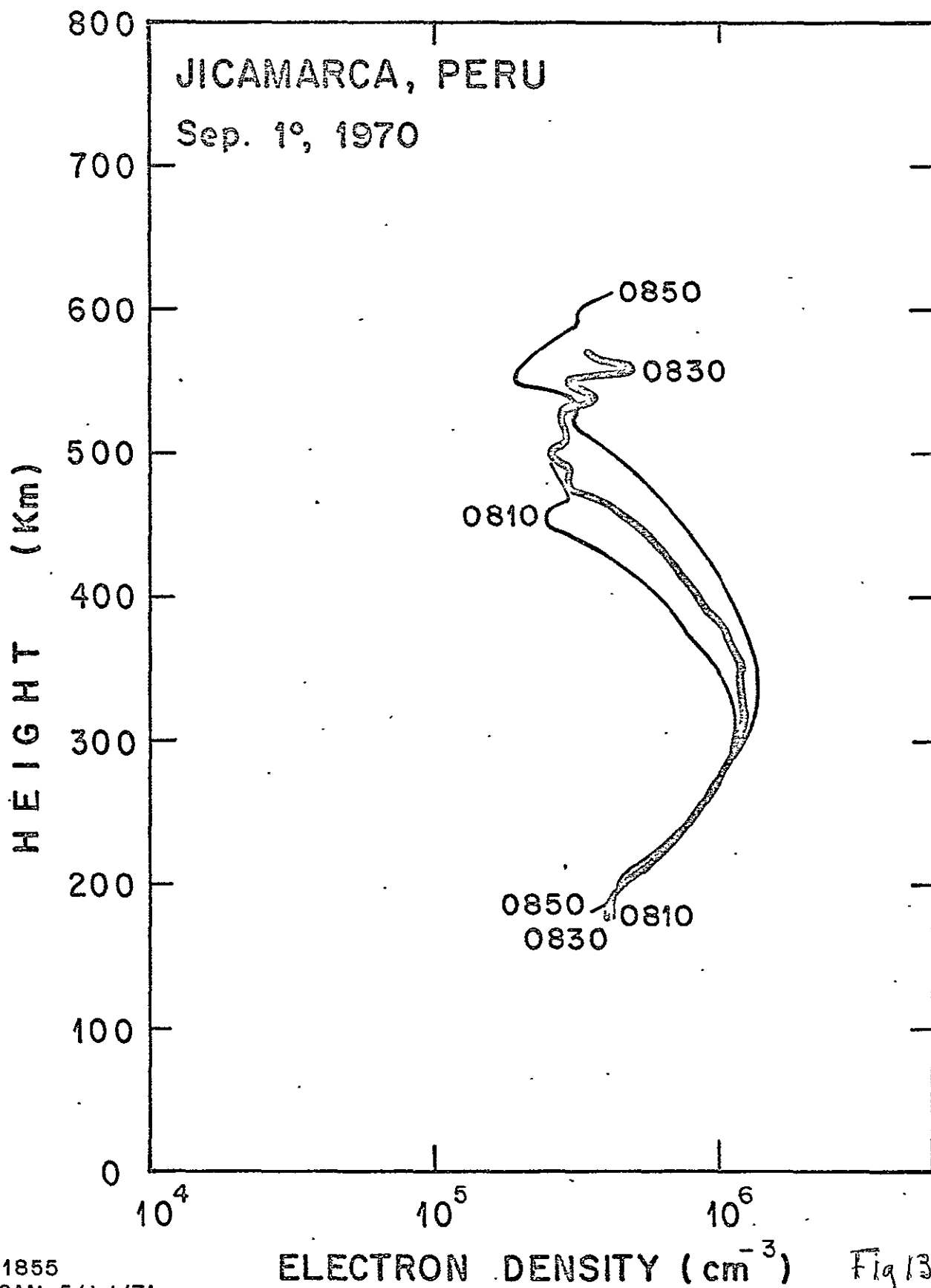


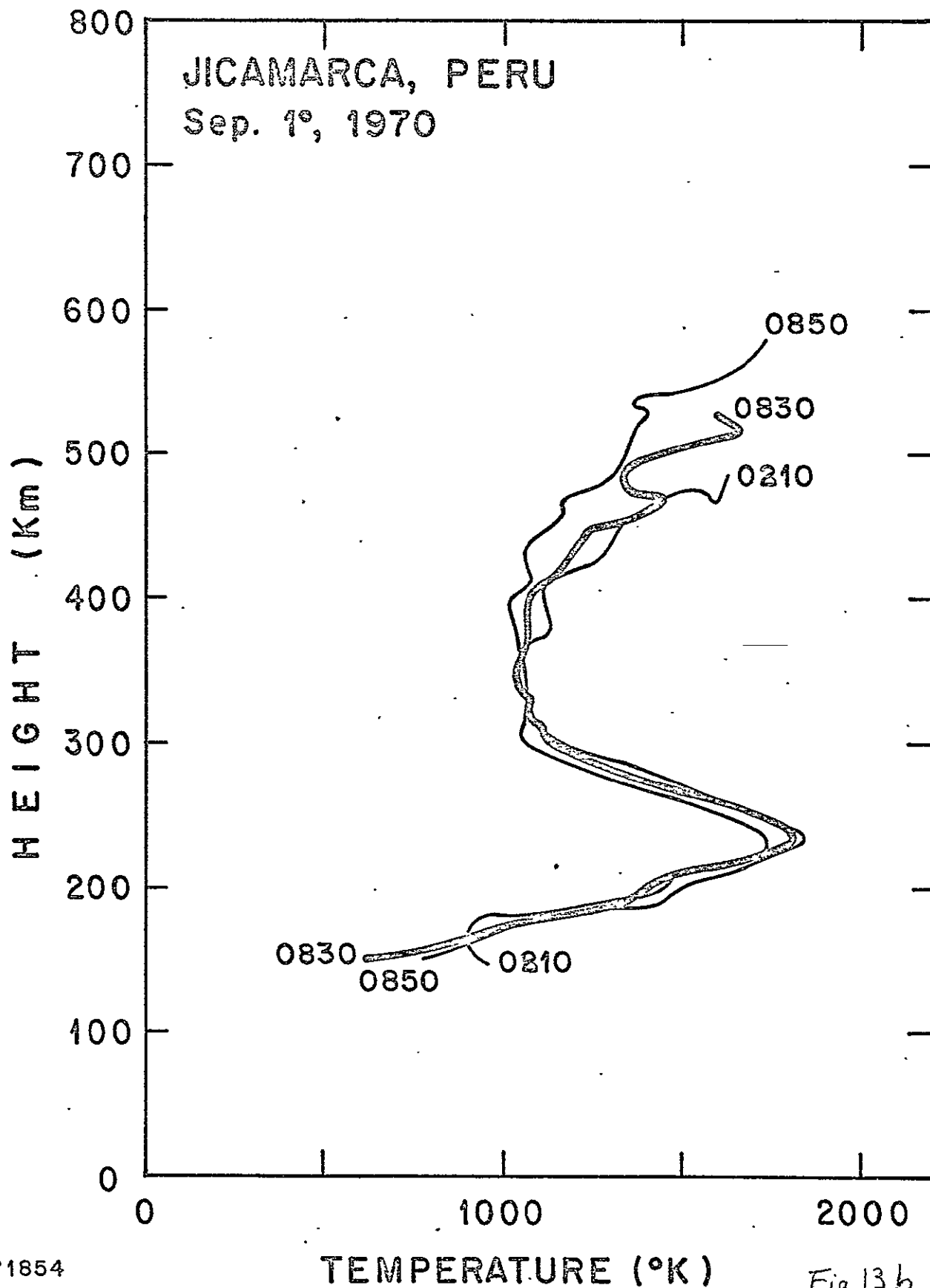
Nº1850
JICAM-2/Jul/71
P.L./aloht.

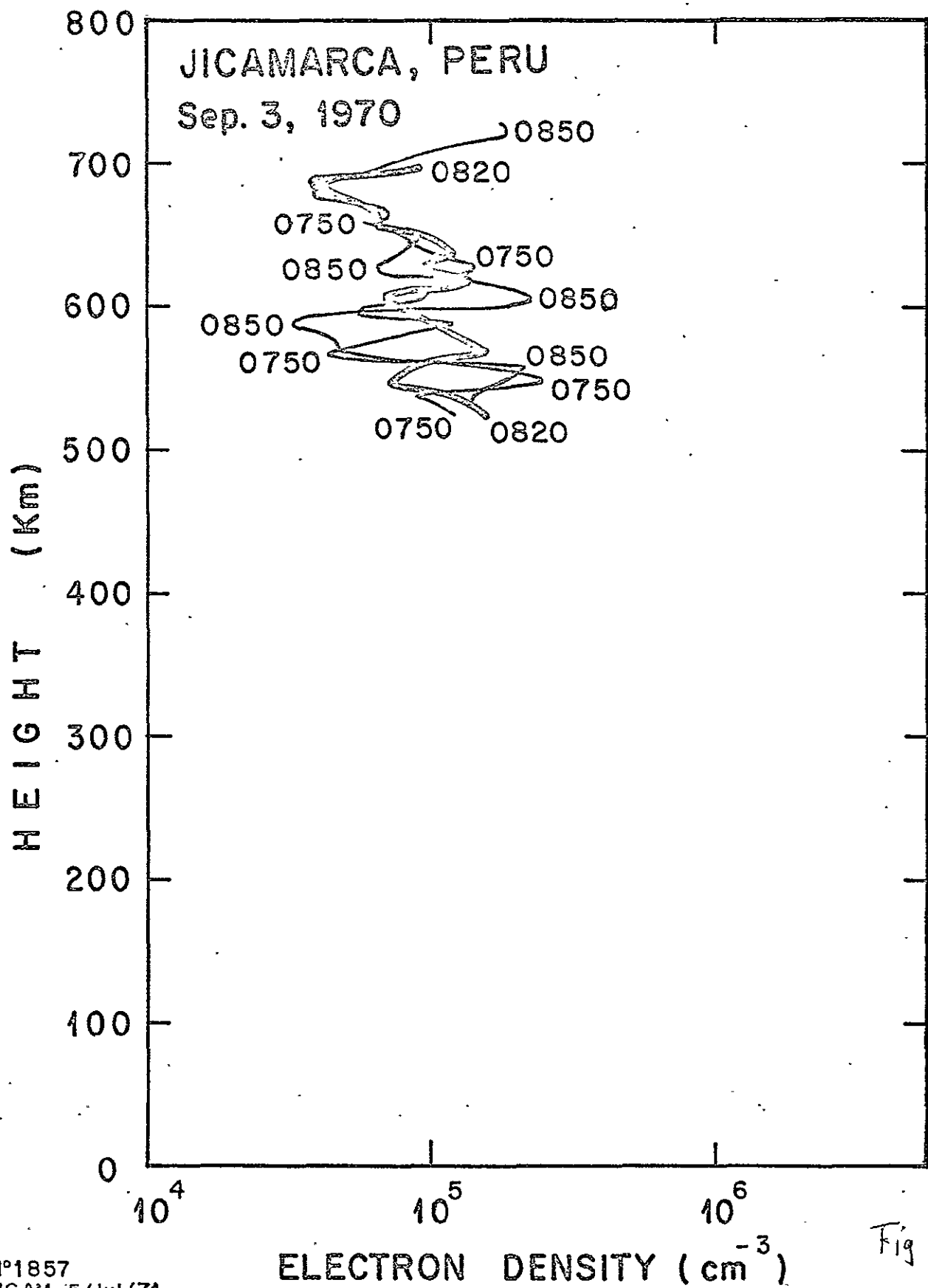
Fig 116

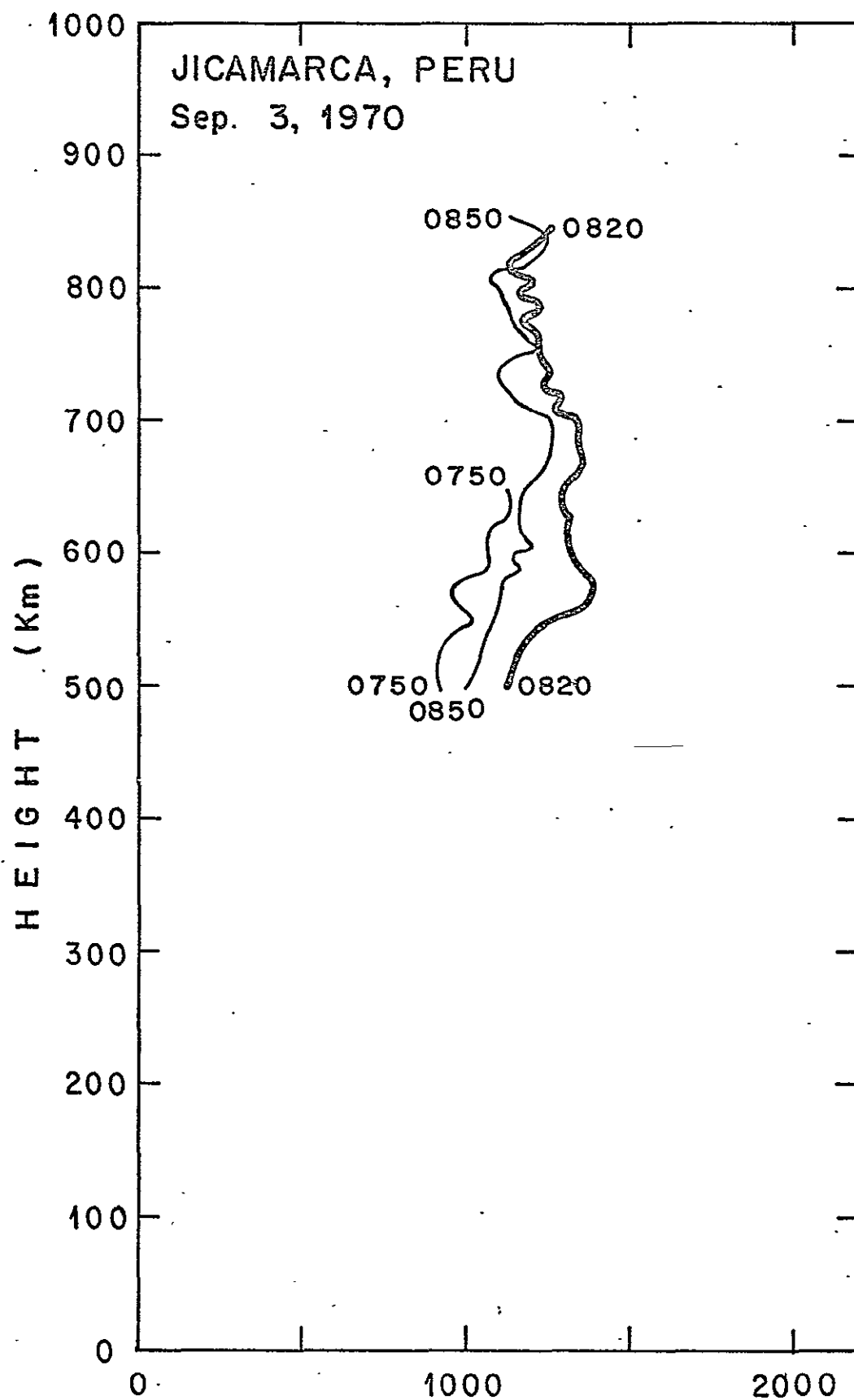


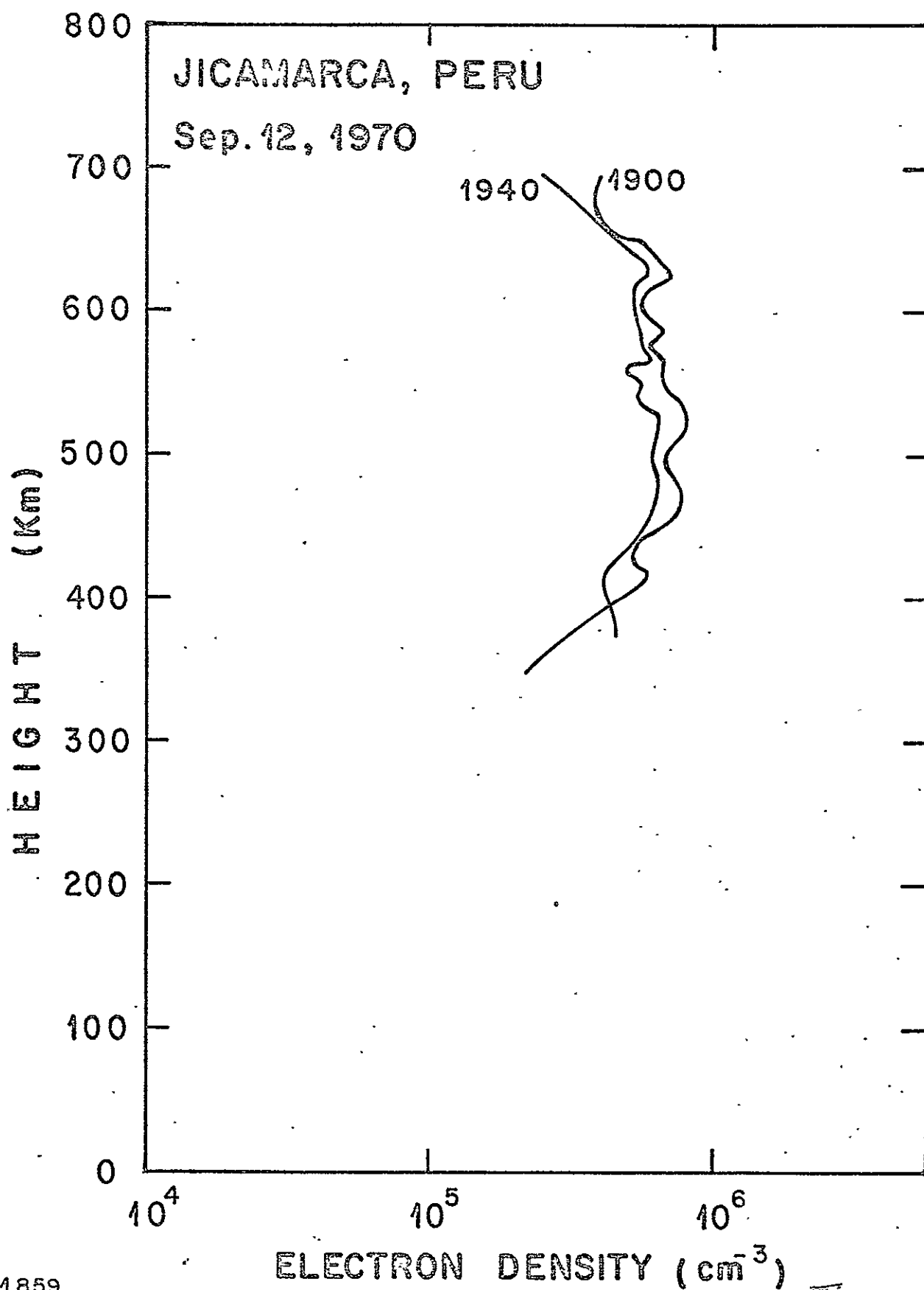






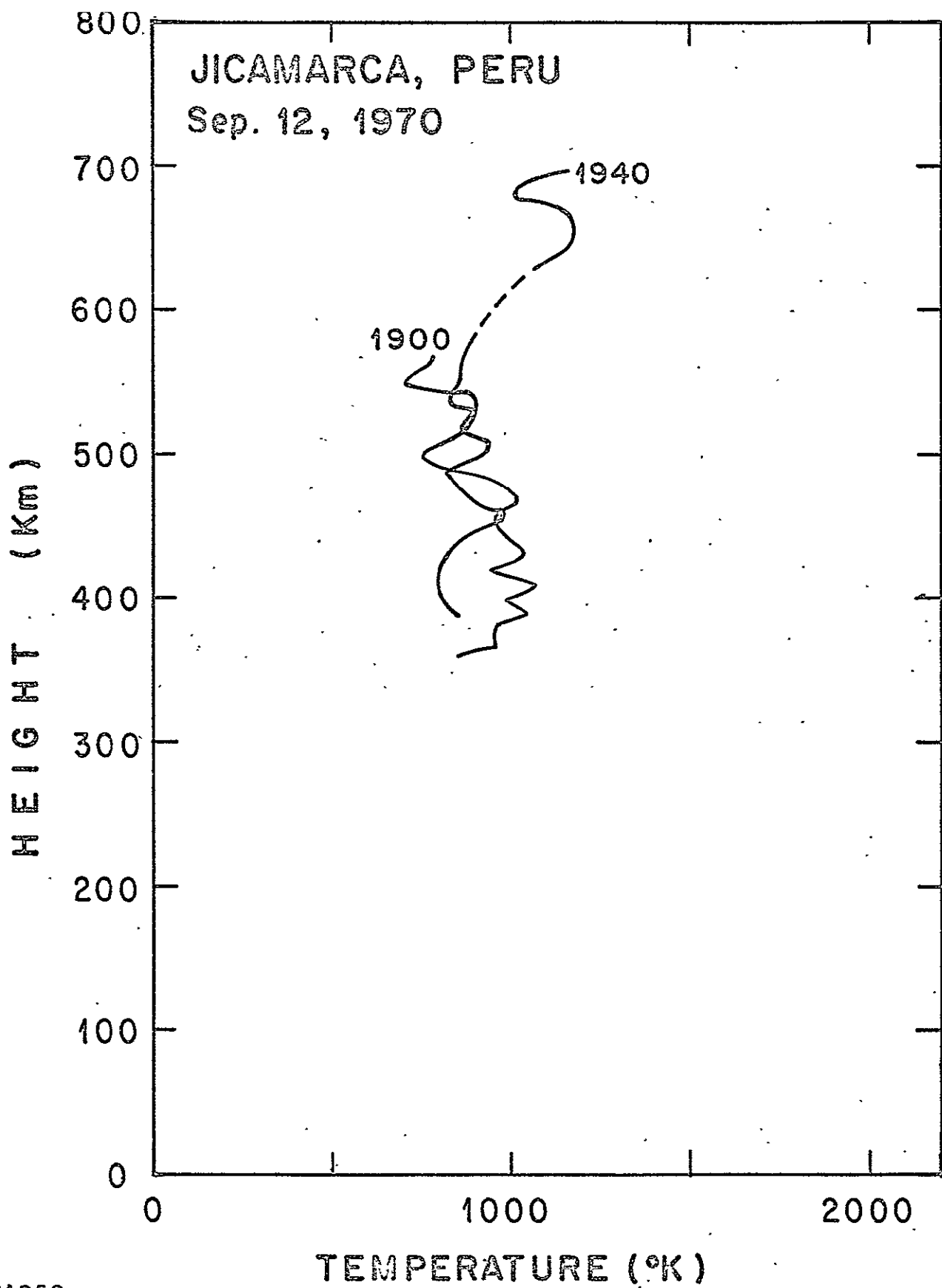


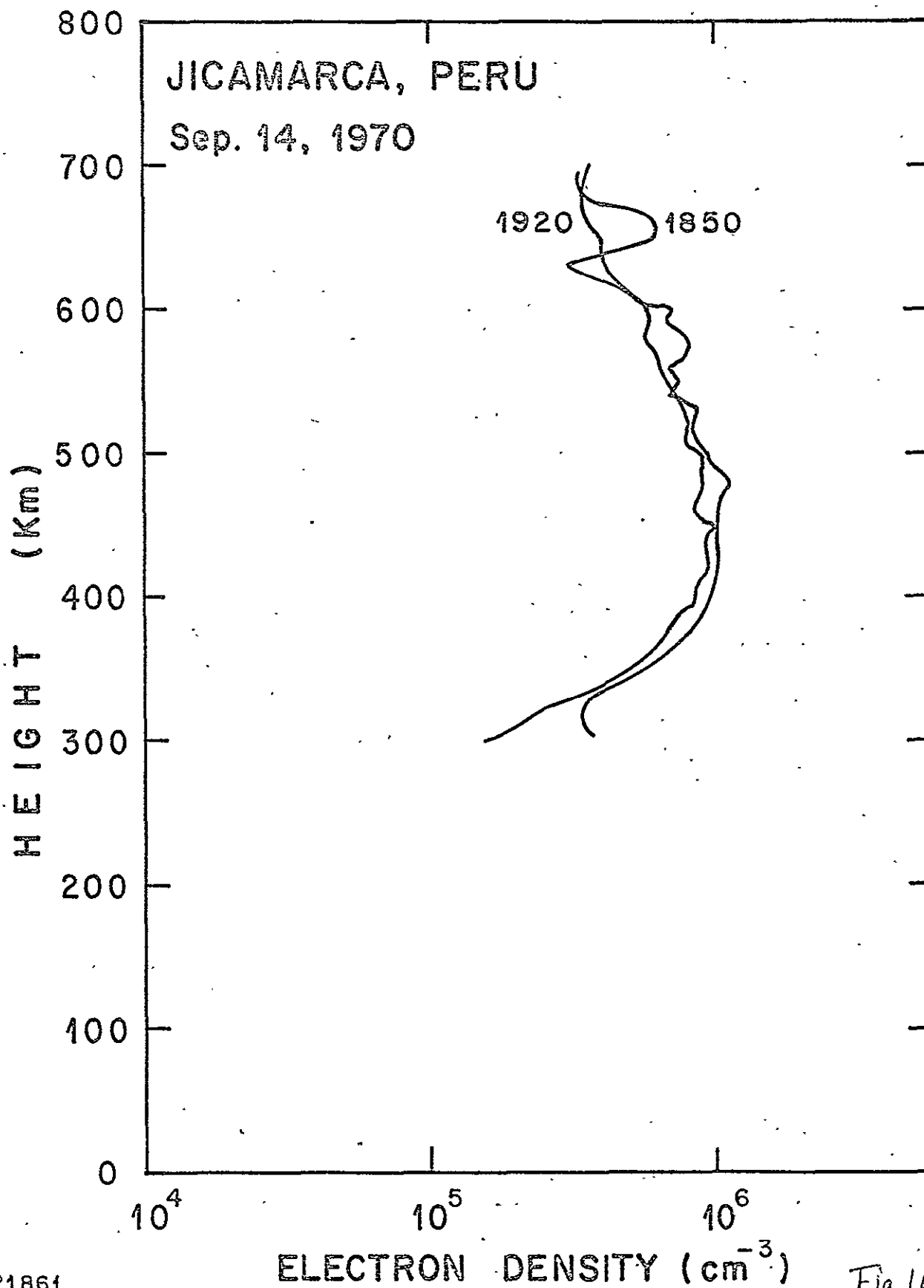


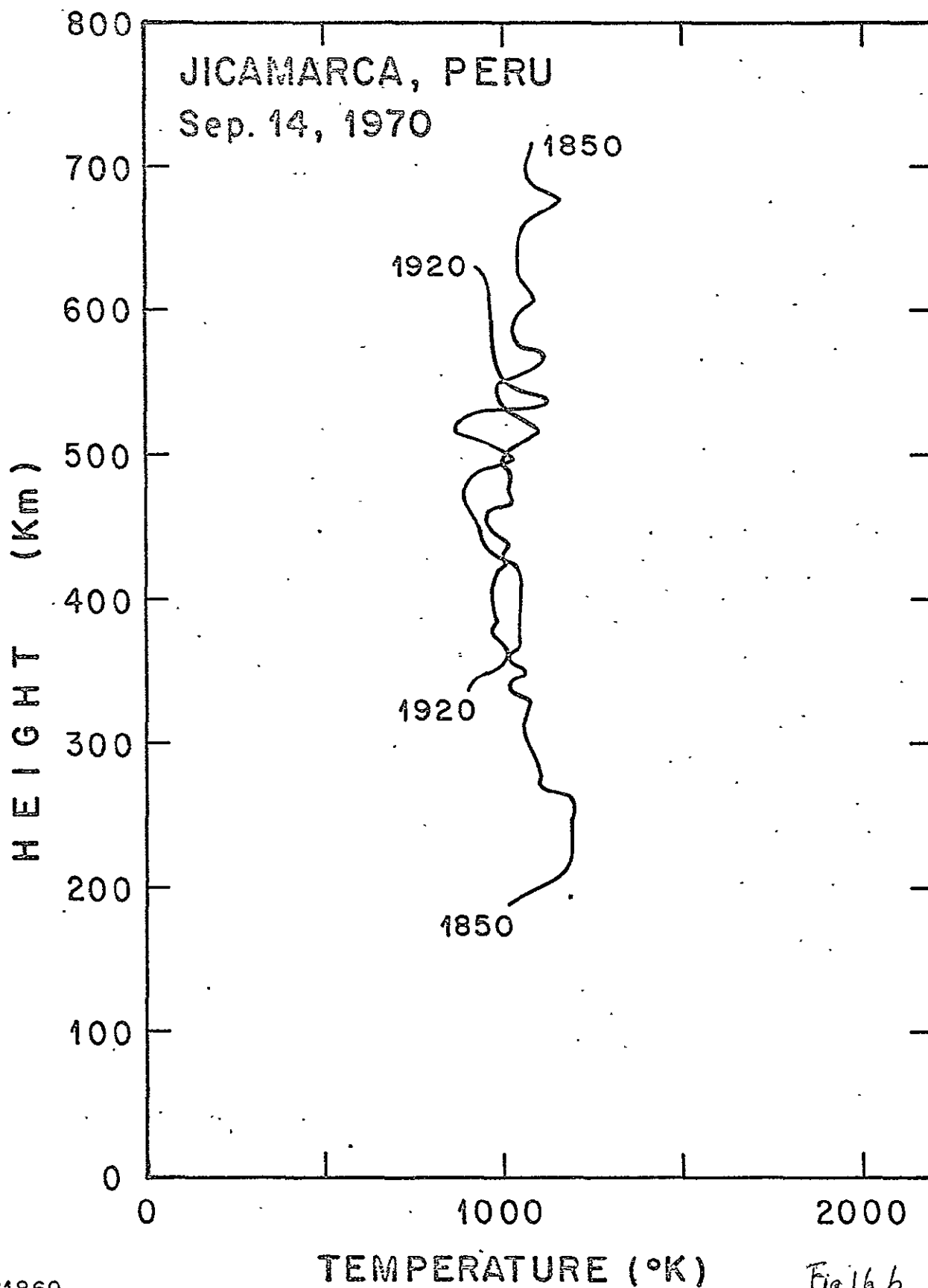


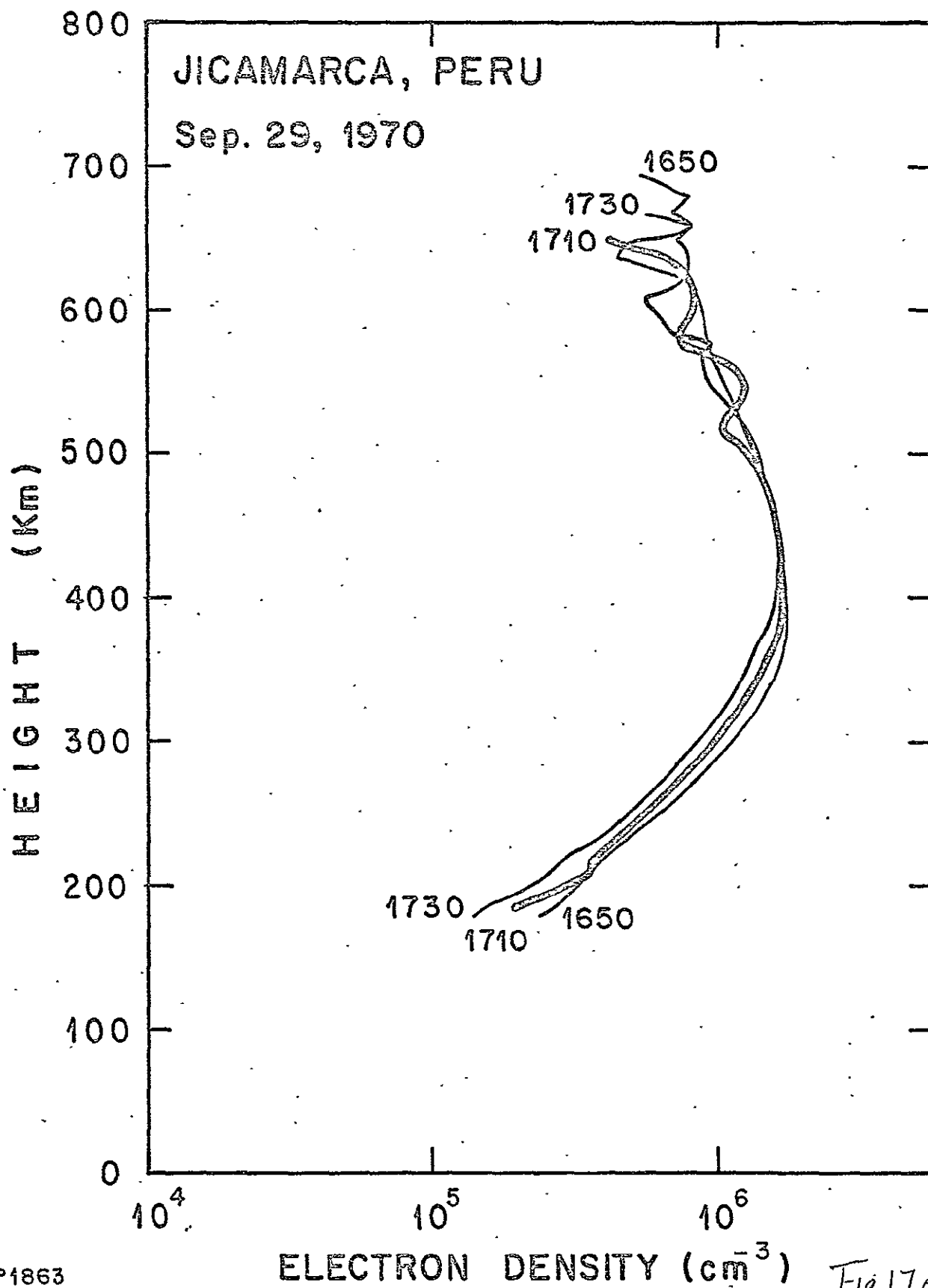
Nº1859
JICAM-6/Jul/71
P.L./aloht.

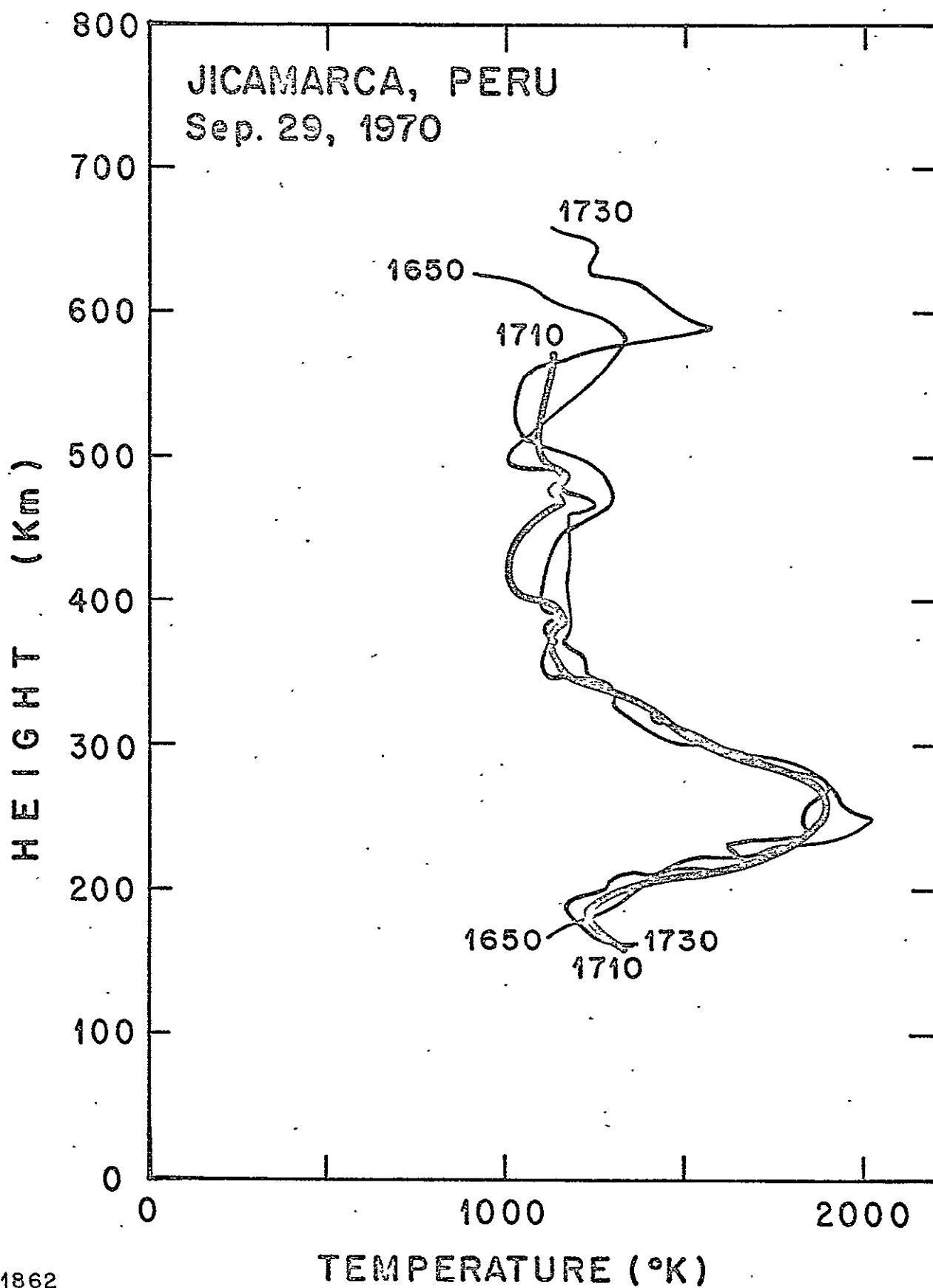
Fig 15a

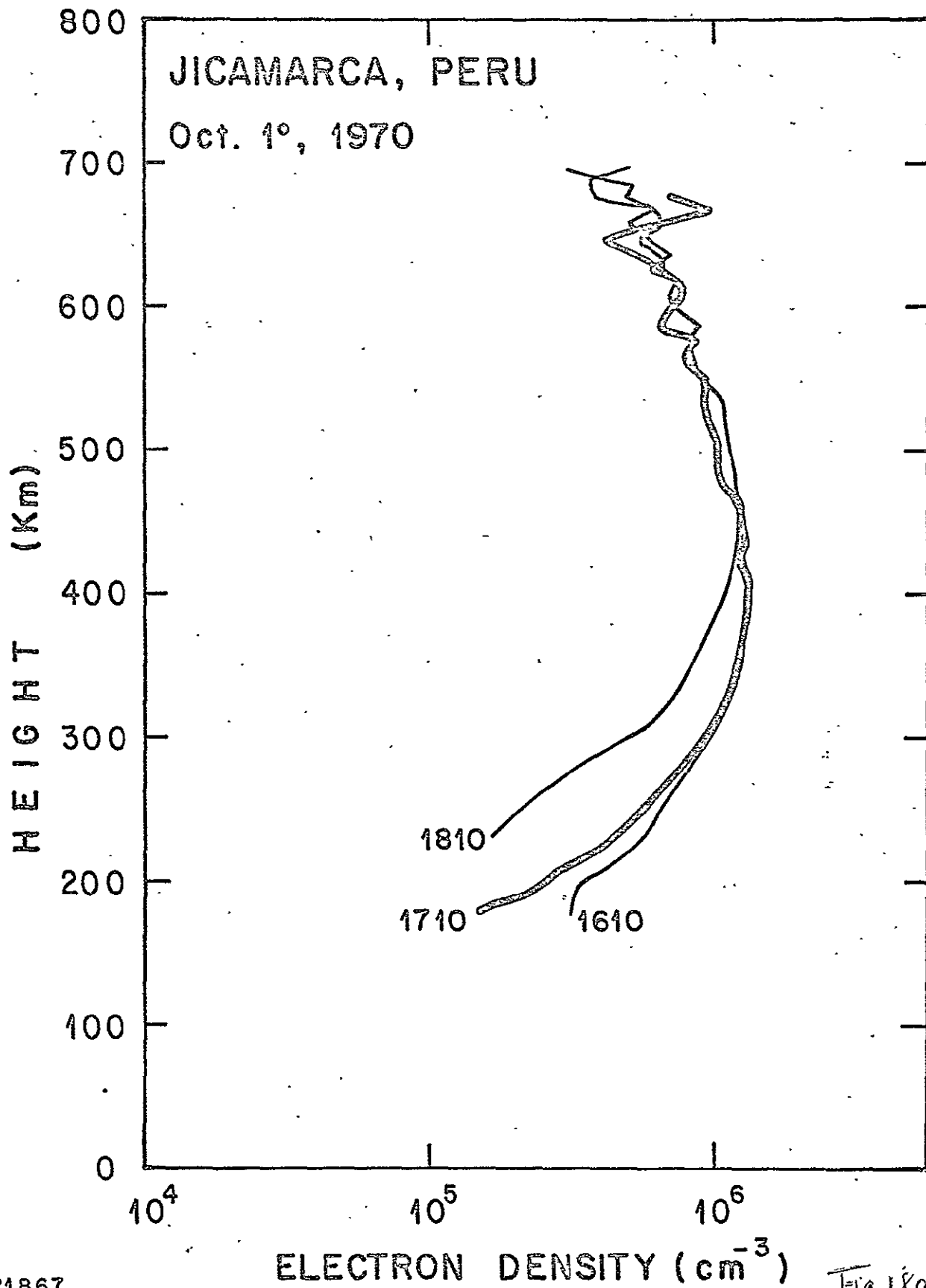


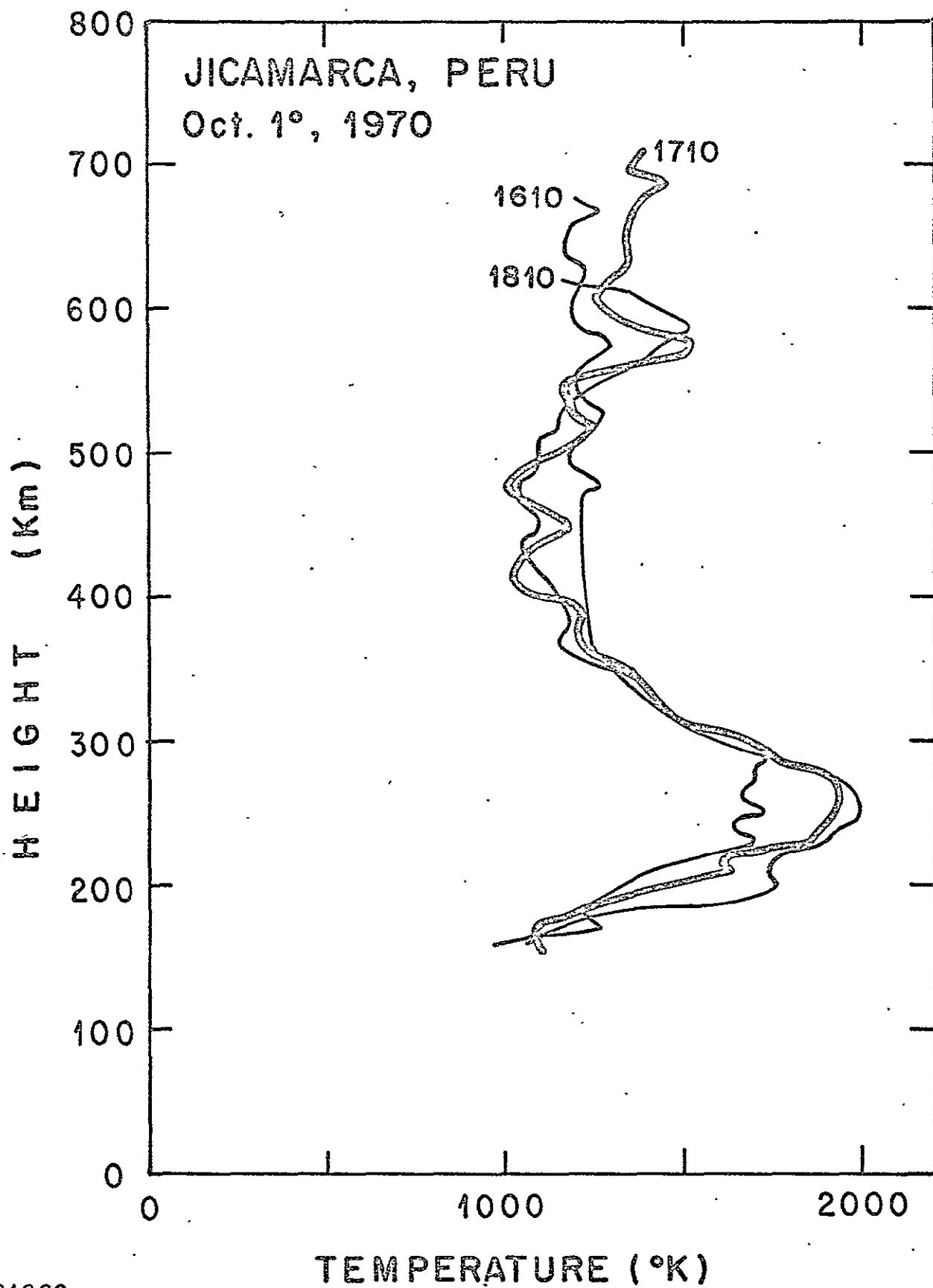






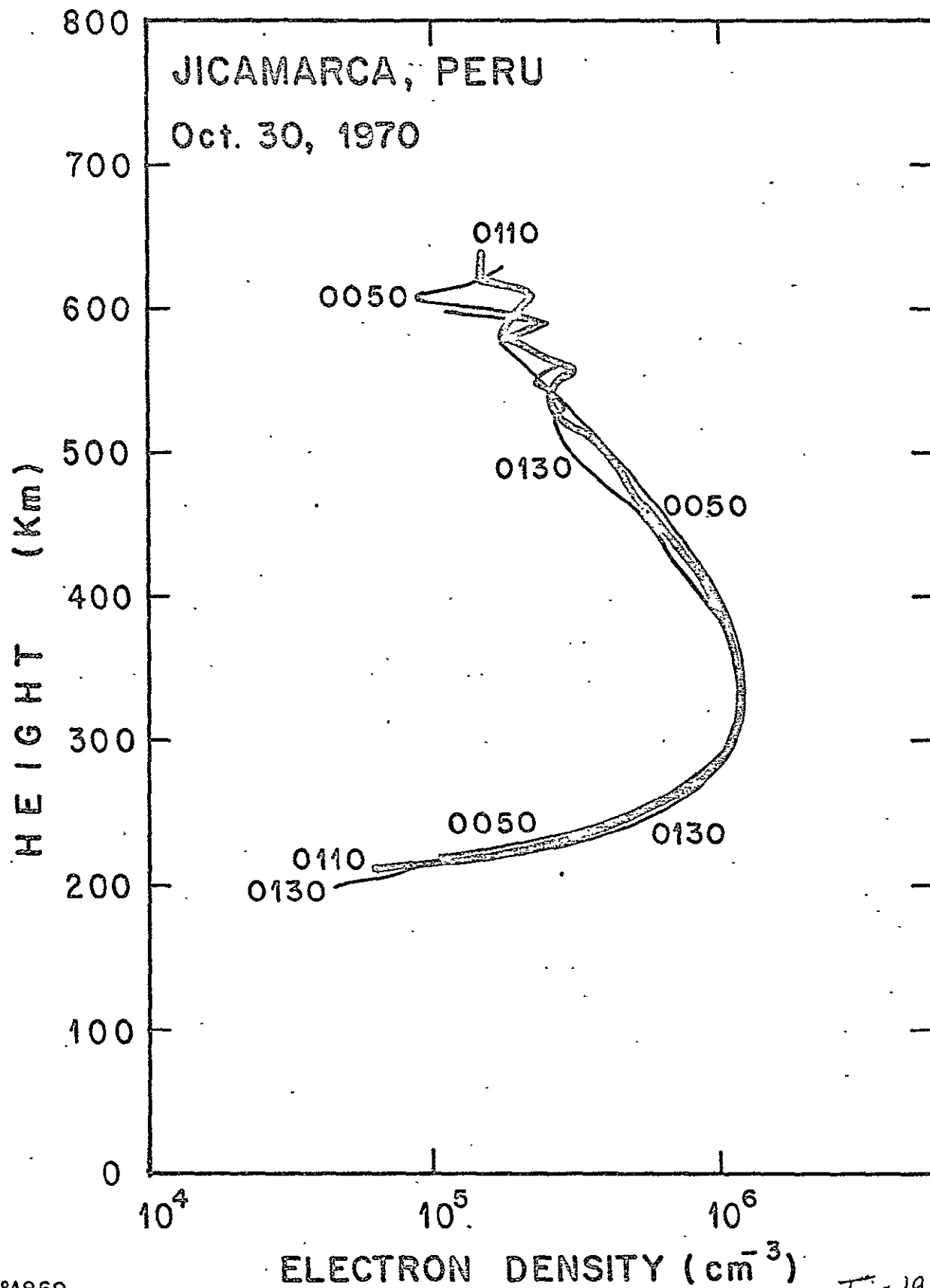


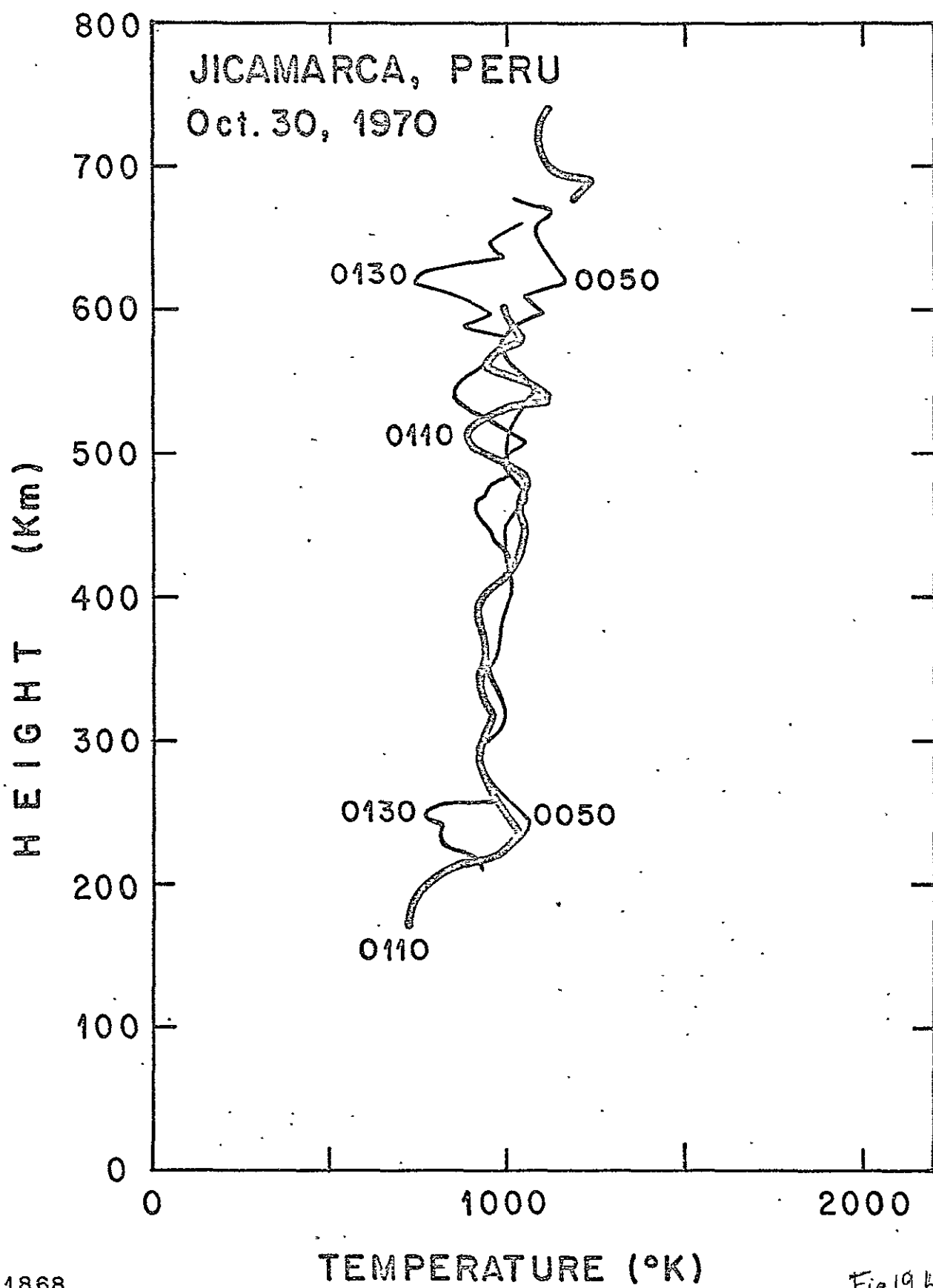


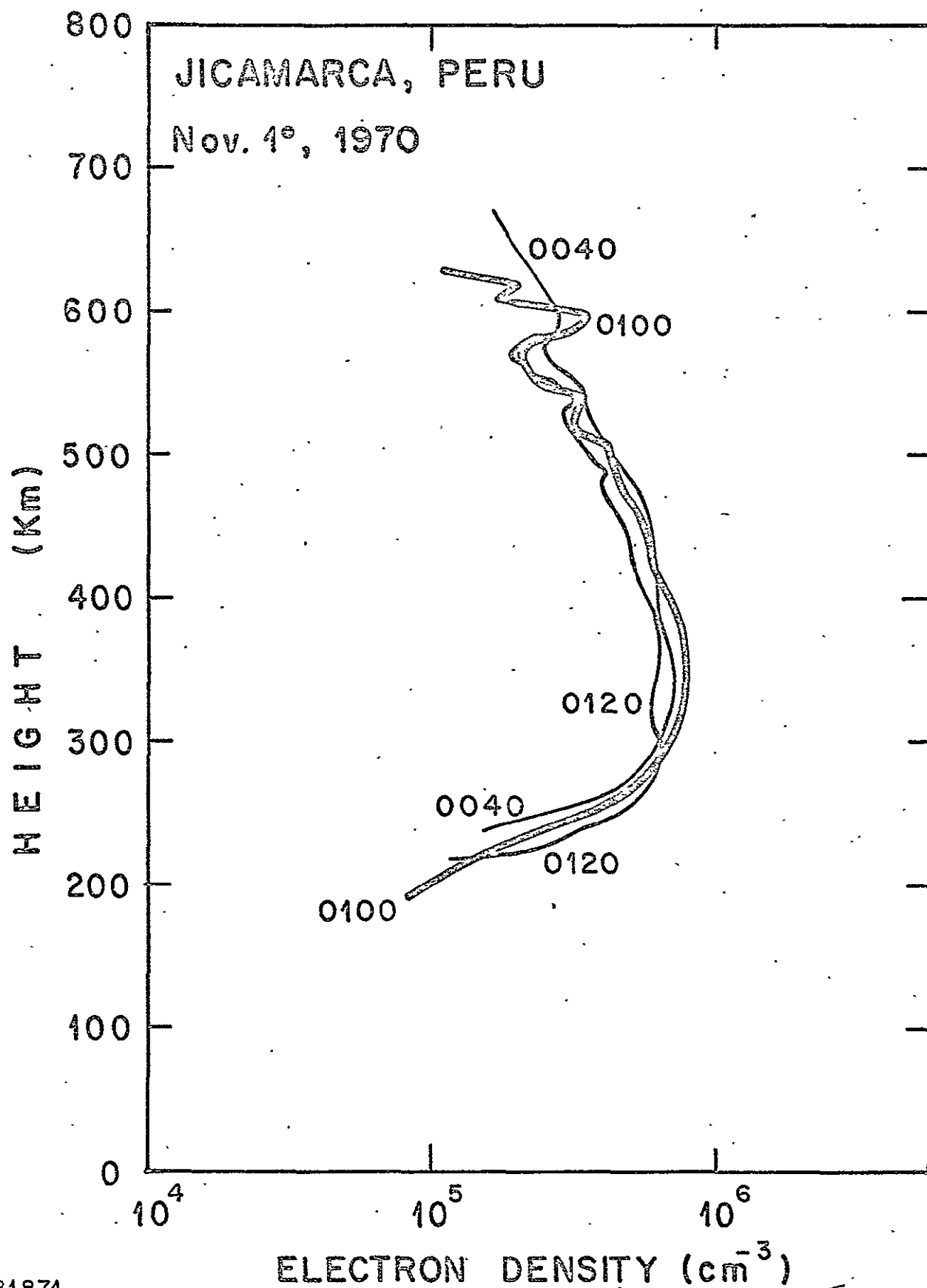


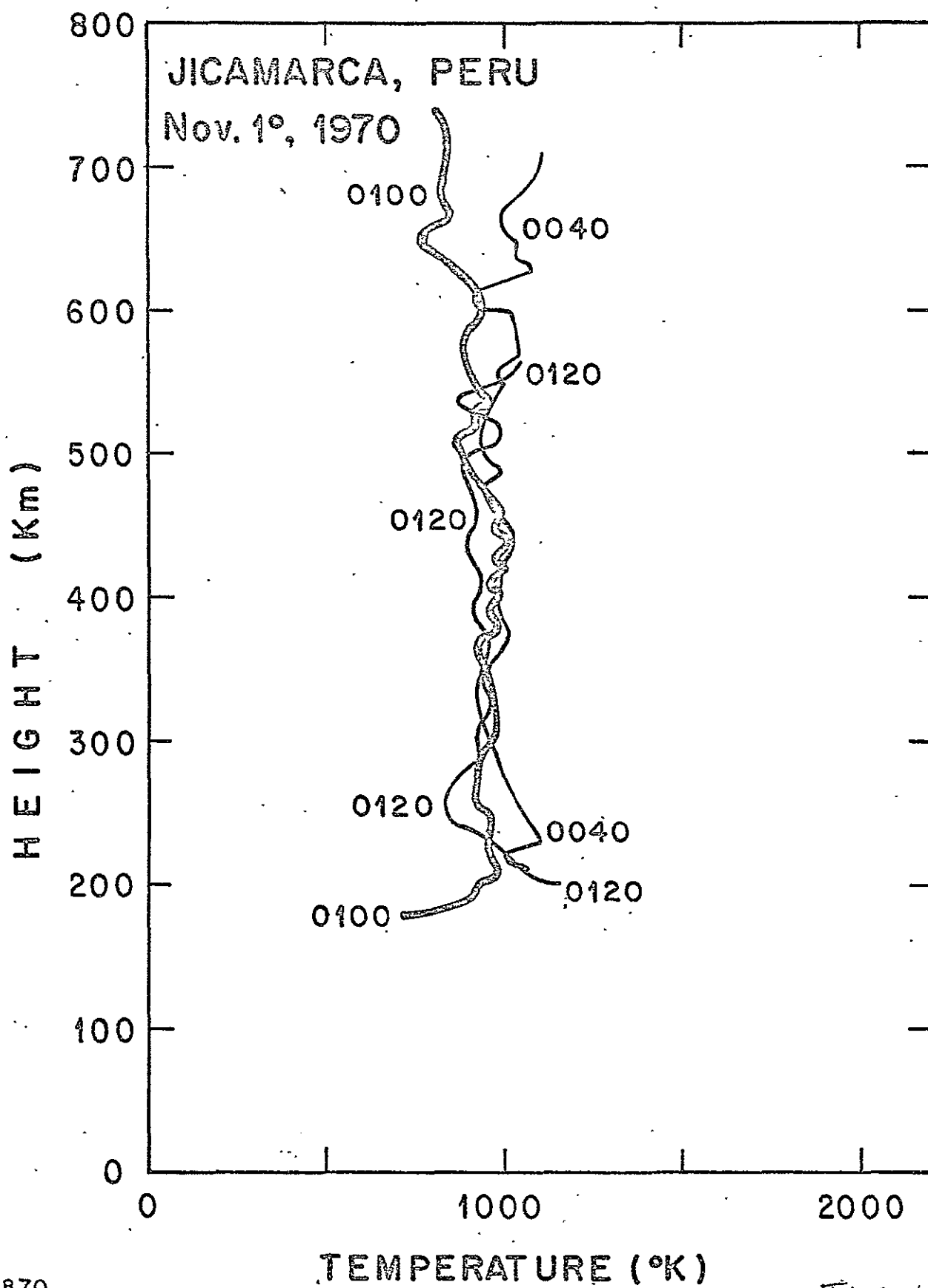
N°1866
JICAM-8/Jul/71
P. L. /aloh.t.

Fig 18b







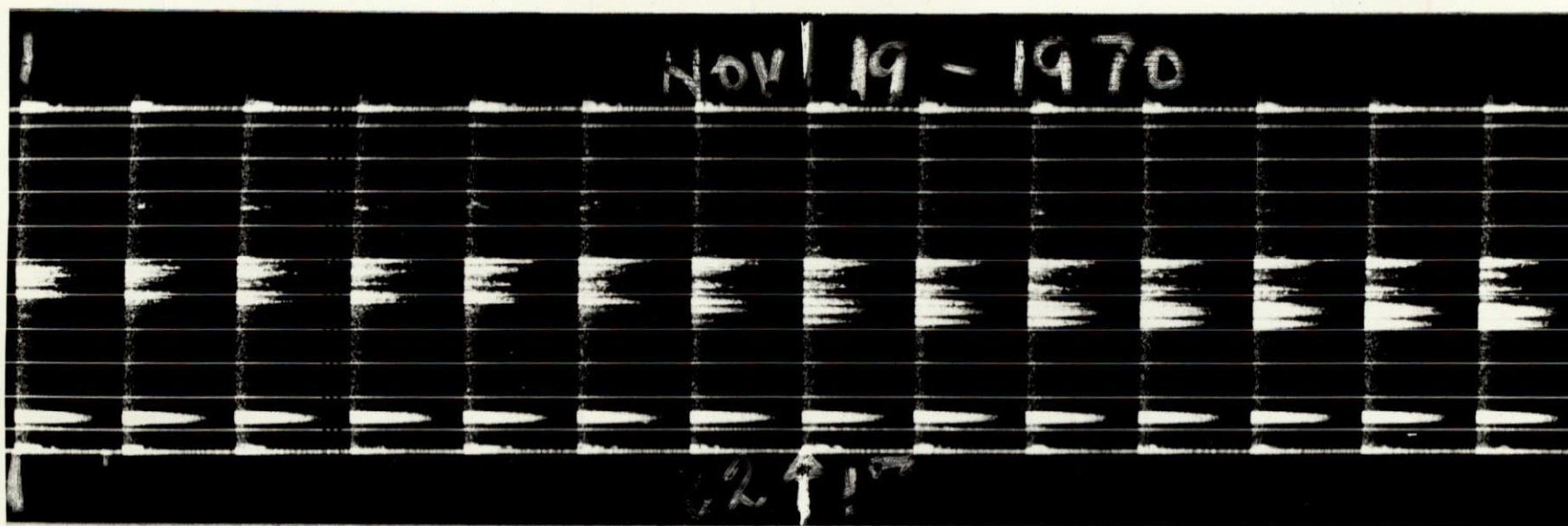


N°1870
JICAM-9/Jul /71
P. L. /aloht.

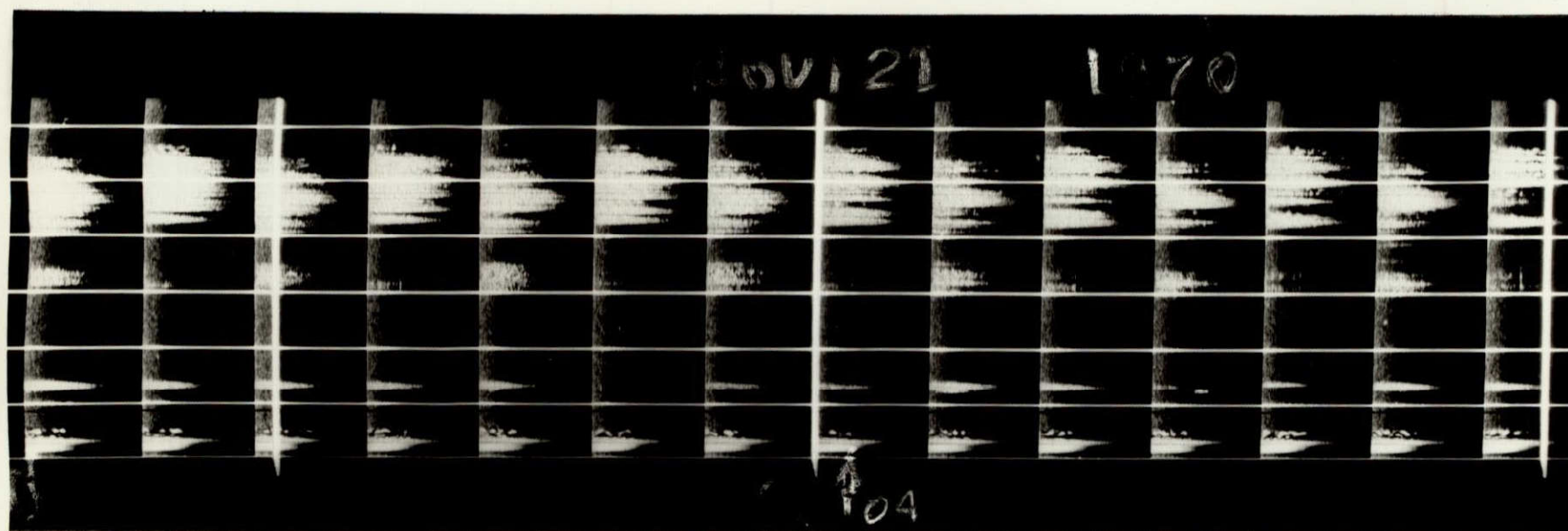
Fig 20 b

APPENDIX II

SPREAD-F OBSERVATIONS CO-ORDINATED WITH OGO-VI PASSES



NOT REPRODUCIBLE



NOT REPRODUCIBLE



NOT REPRODUCIBLE

Nov | 25 197

21 34

21 37

NOT REPRODUCIBLE

20
④

SEP 10 1970

19 20

NOT REPRODUCIBLE

SEPT 12 1970

19 1/2

NOT REPRODUCIBLE

0507 114 7370

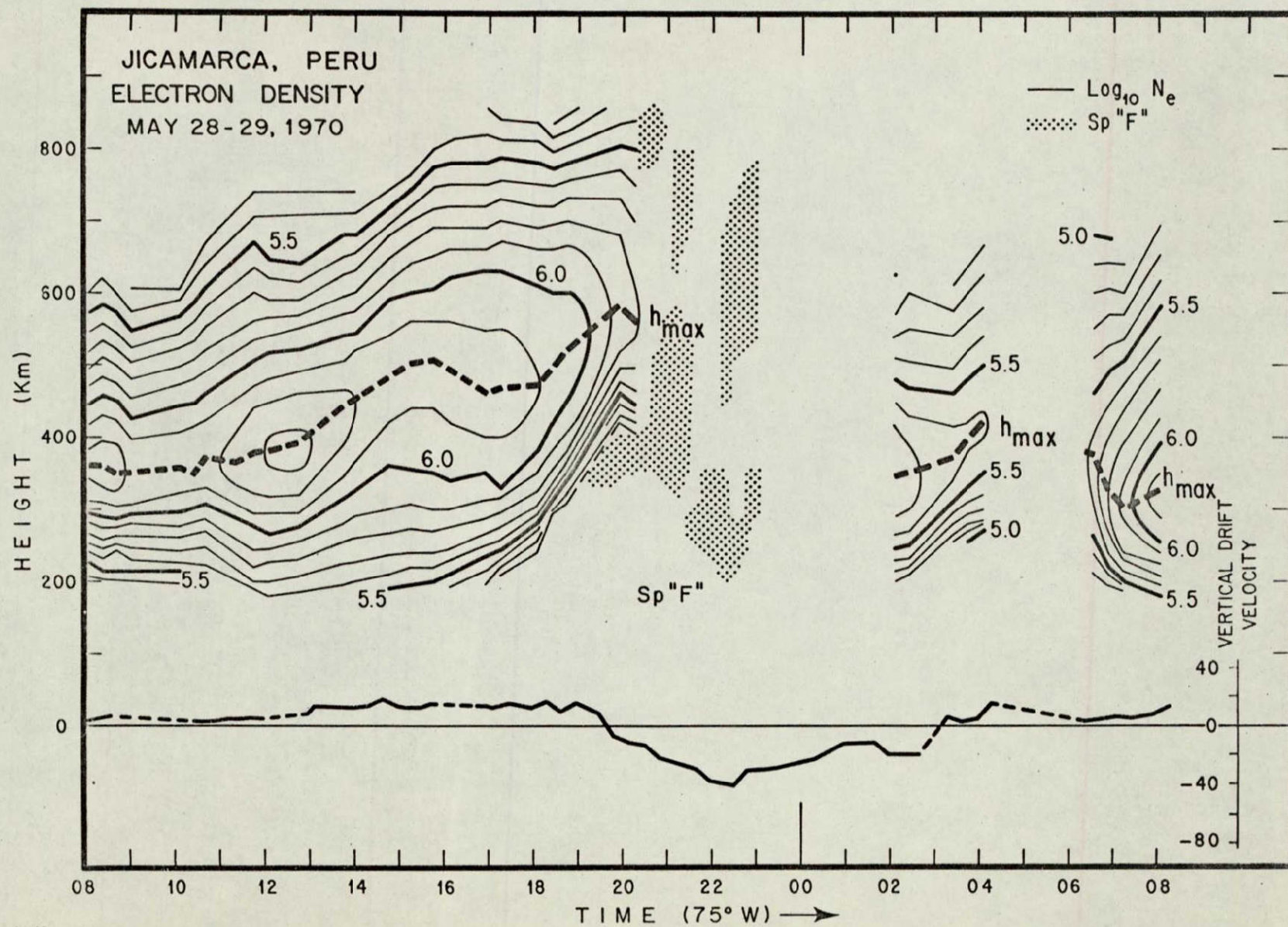
1942

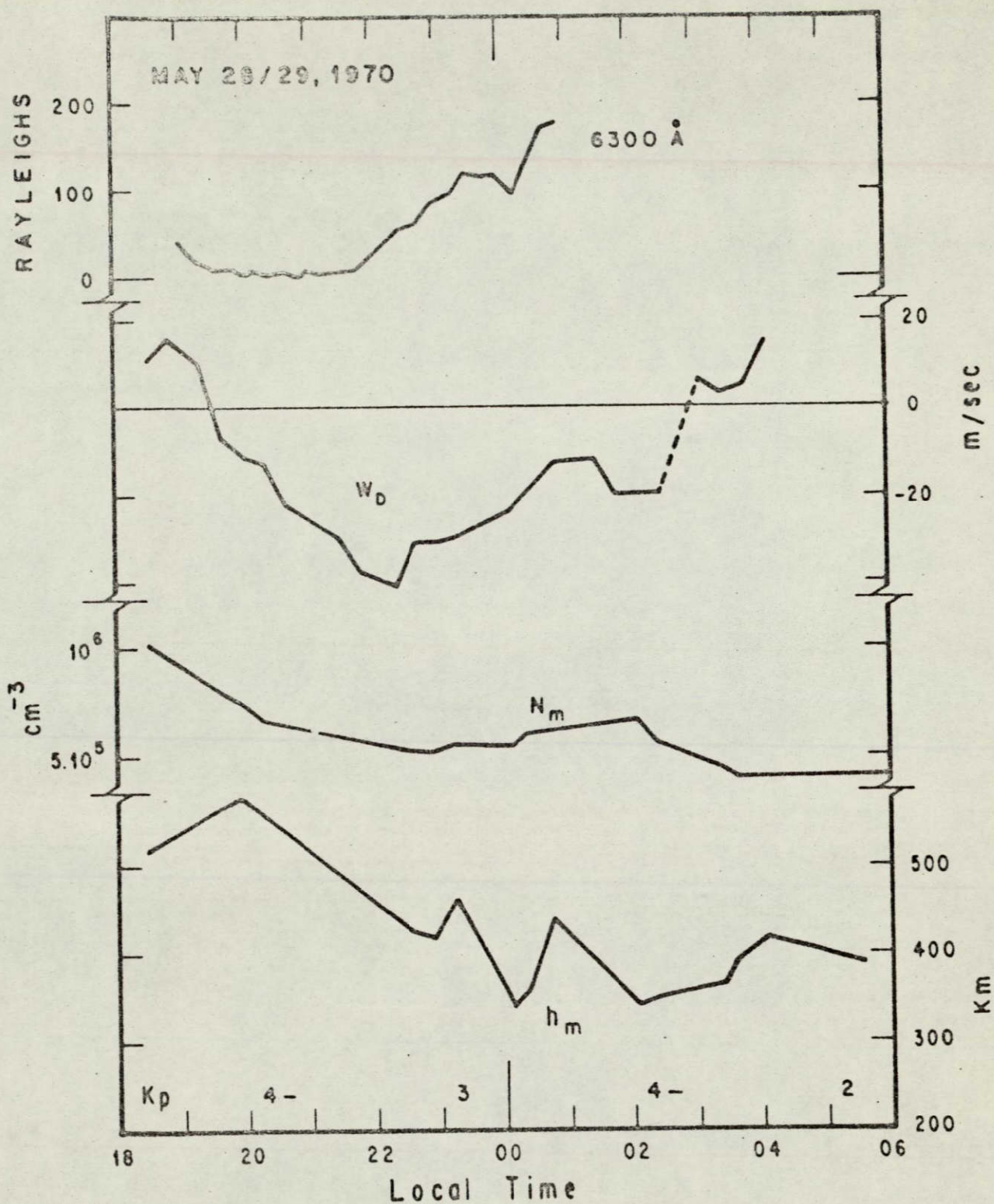
19 104

NOT REPRODUCIBLE

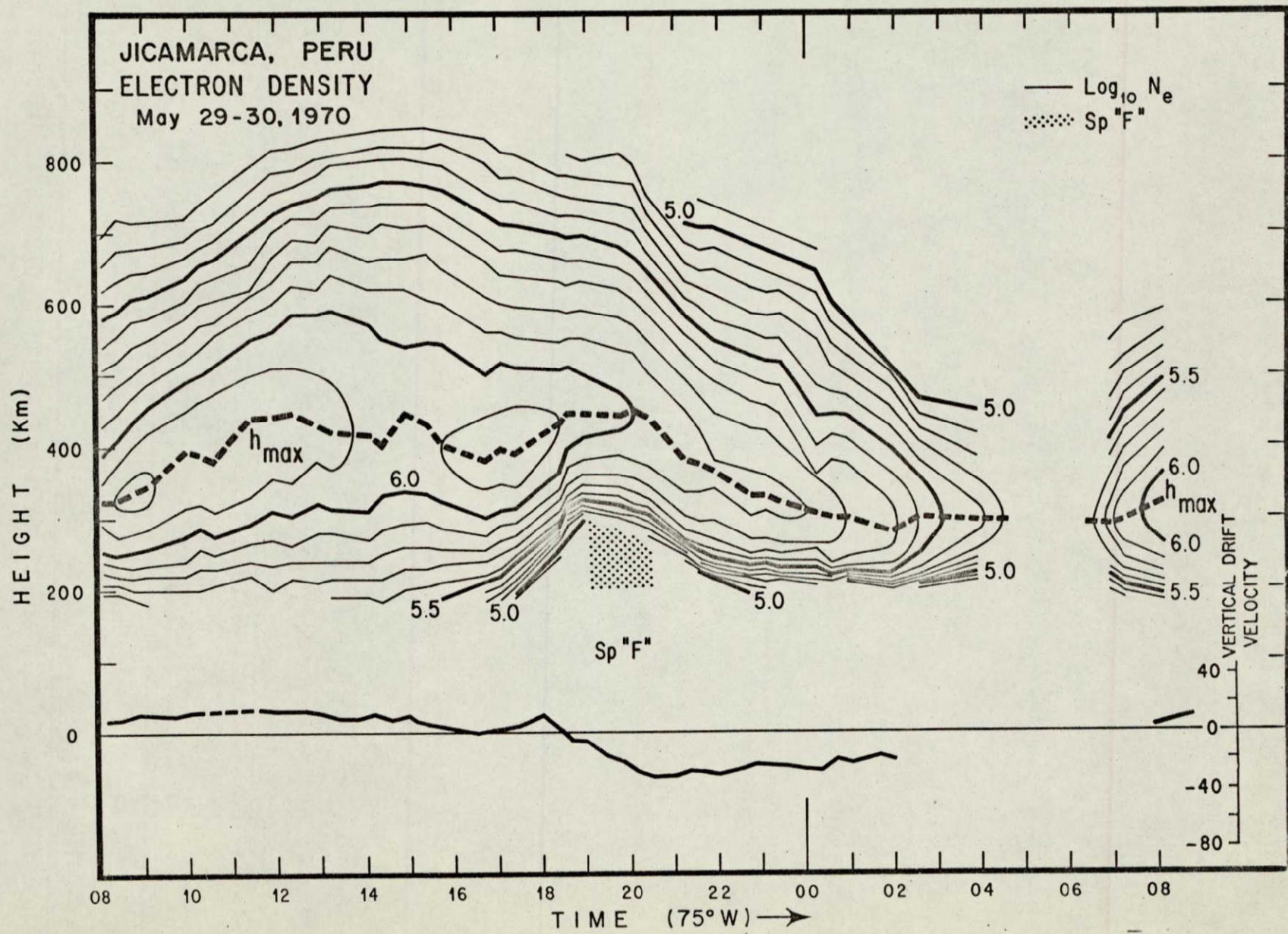
APPENDIX III

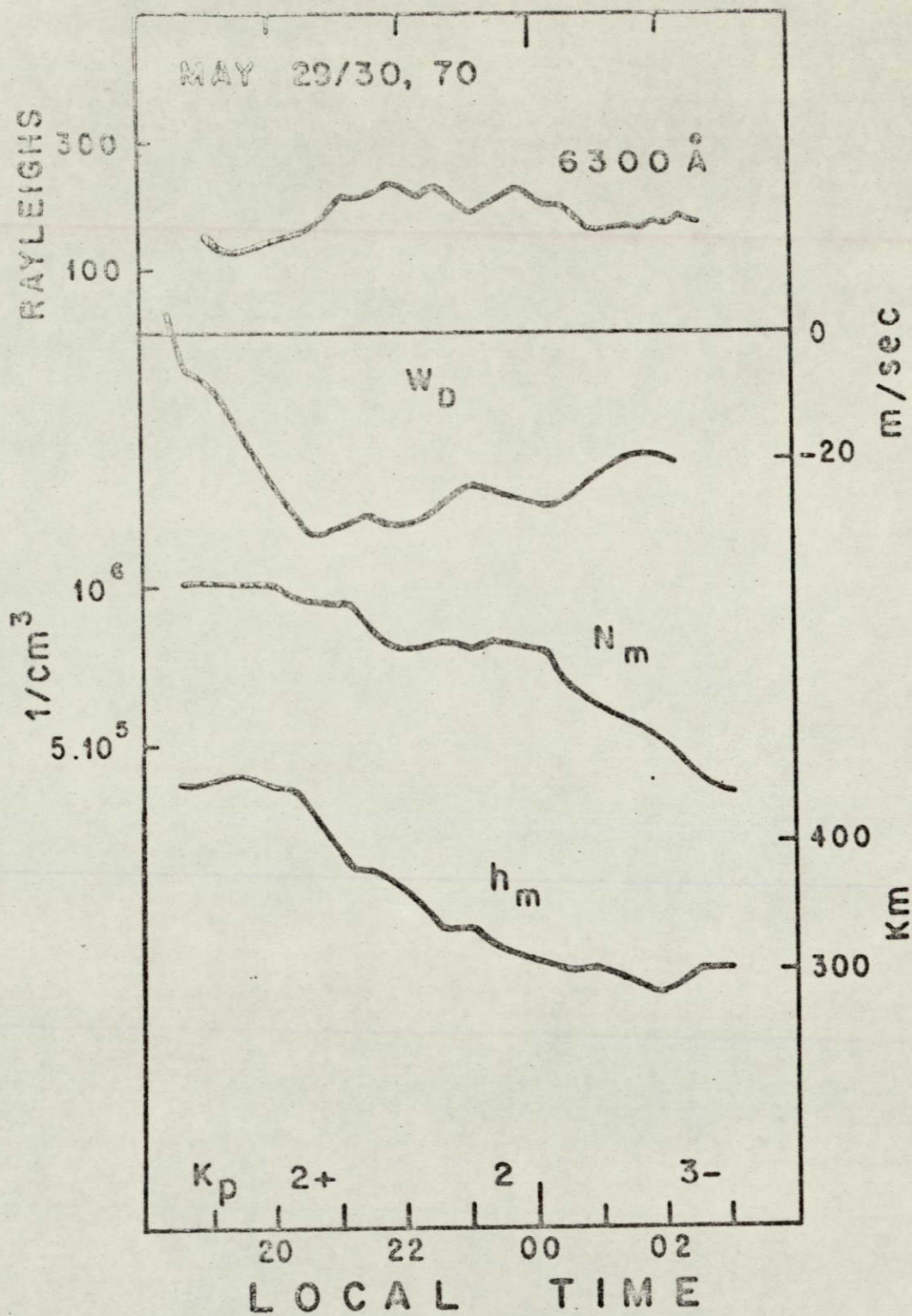
ELECTRON DENSITY CONTOURS, VERTICAL DRIFT, AND 6300 Å⁰ NIGHTGLOW
EMISSION



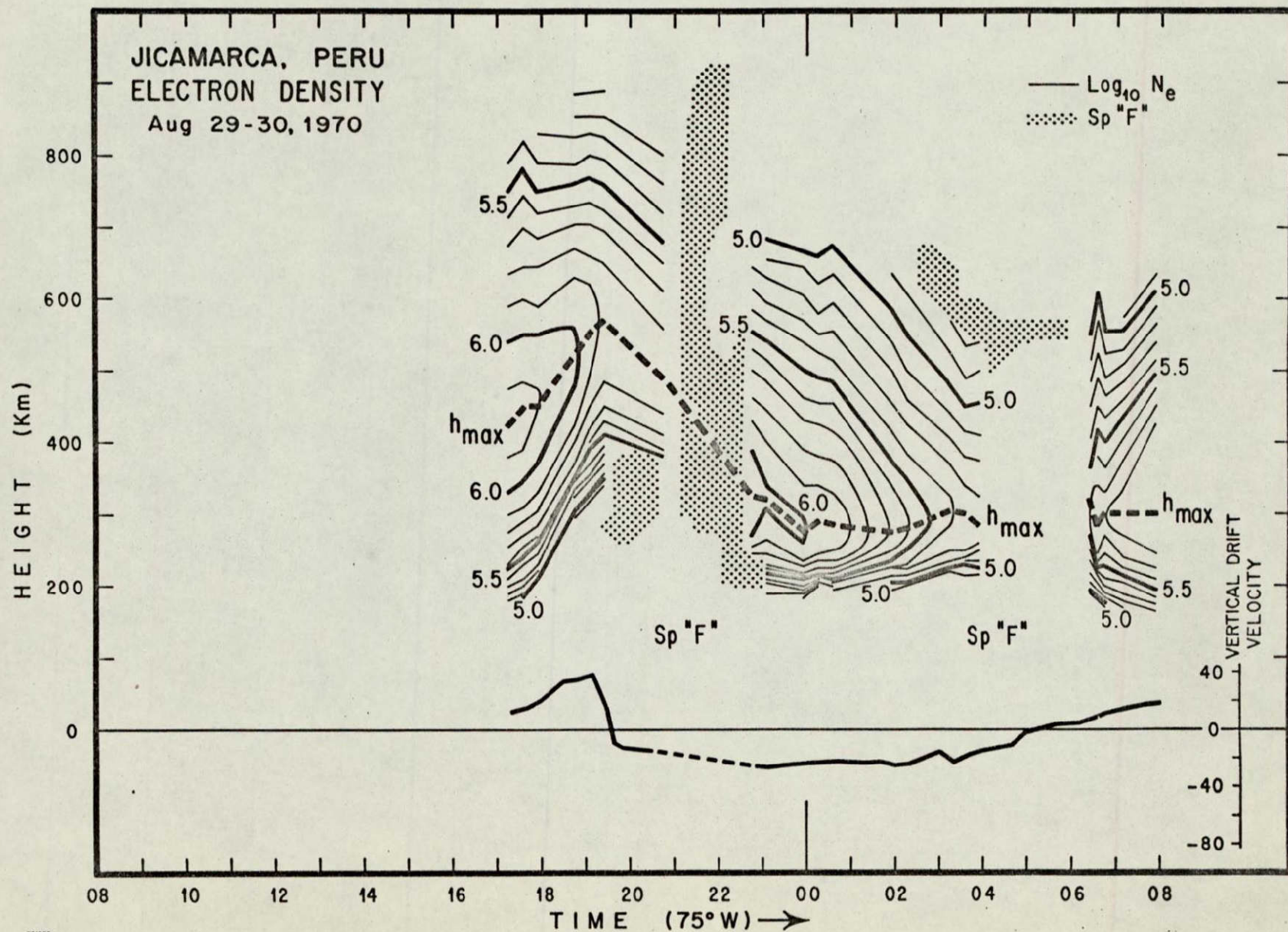


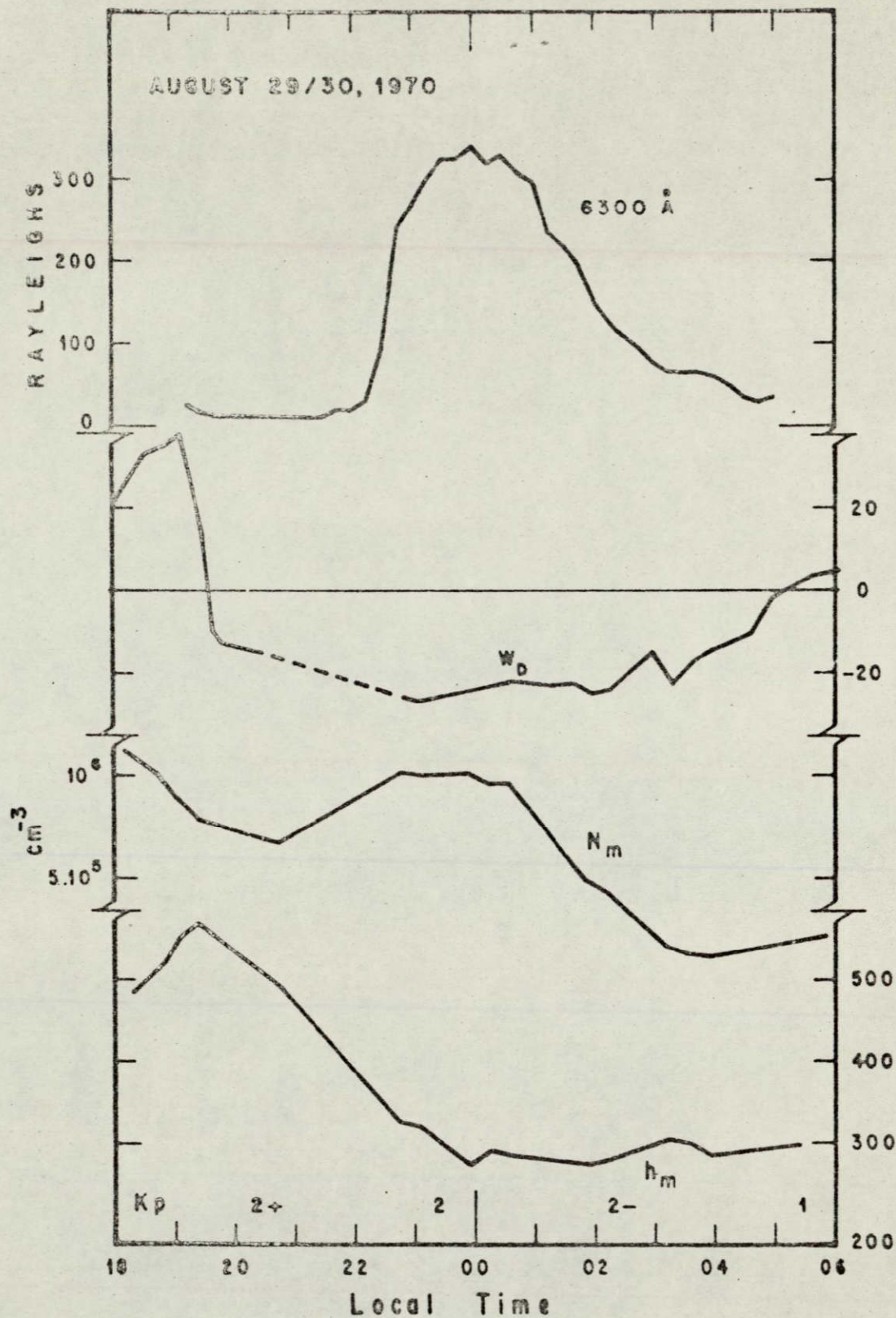
N°1760
JCAM-11/Mar/71
PL /elent

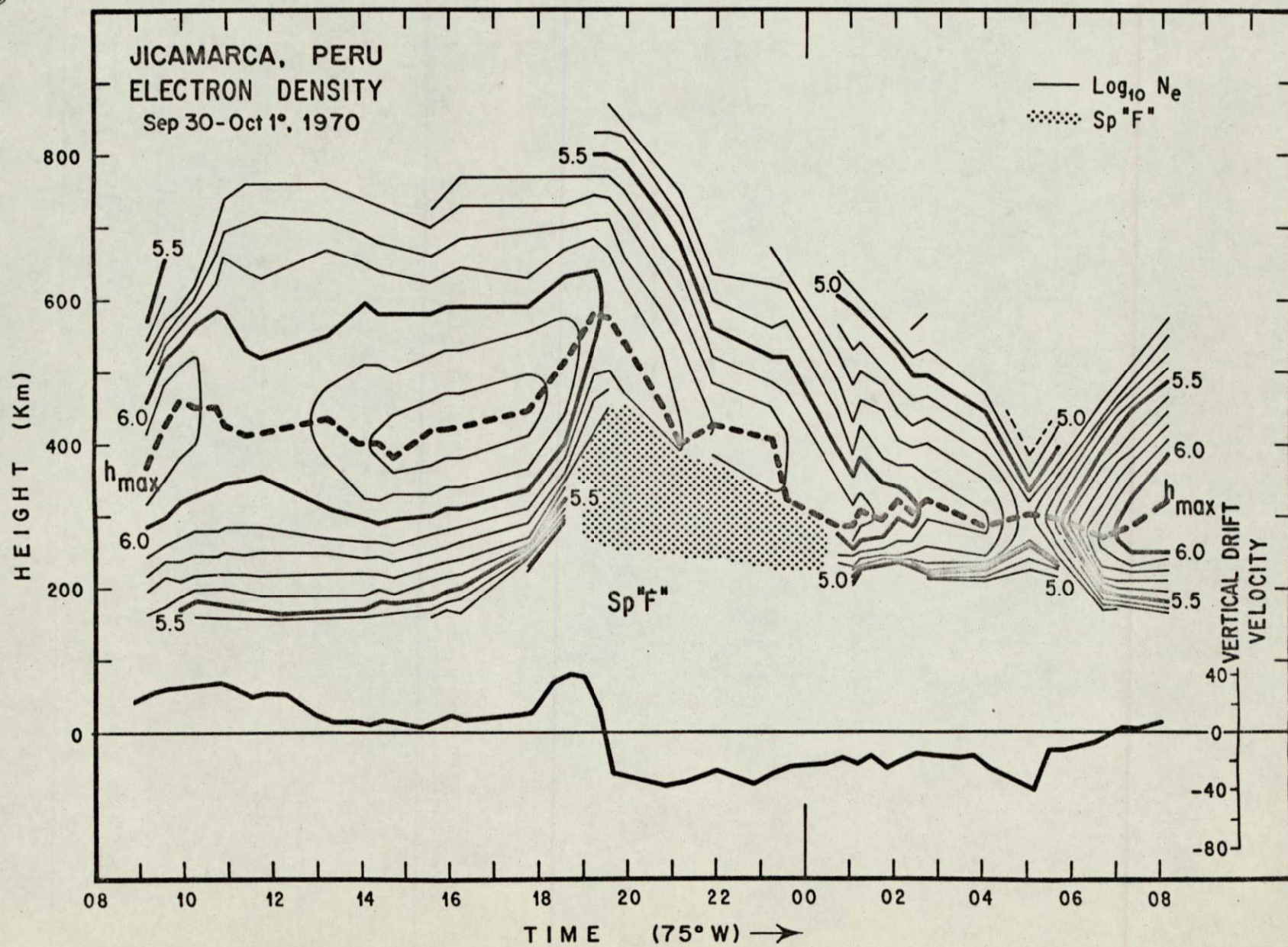


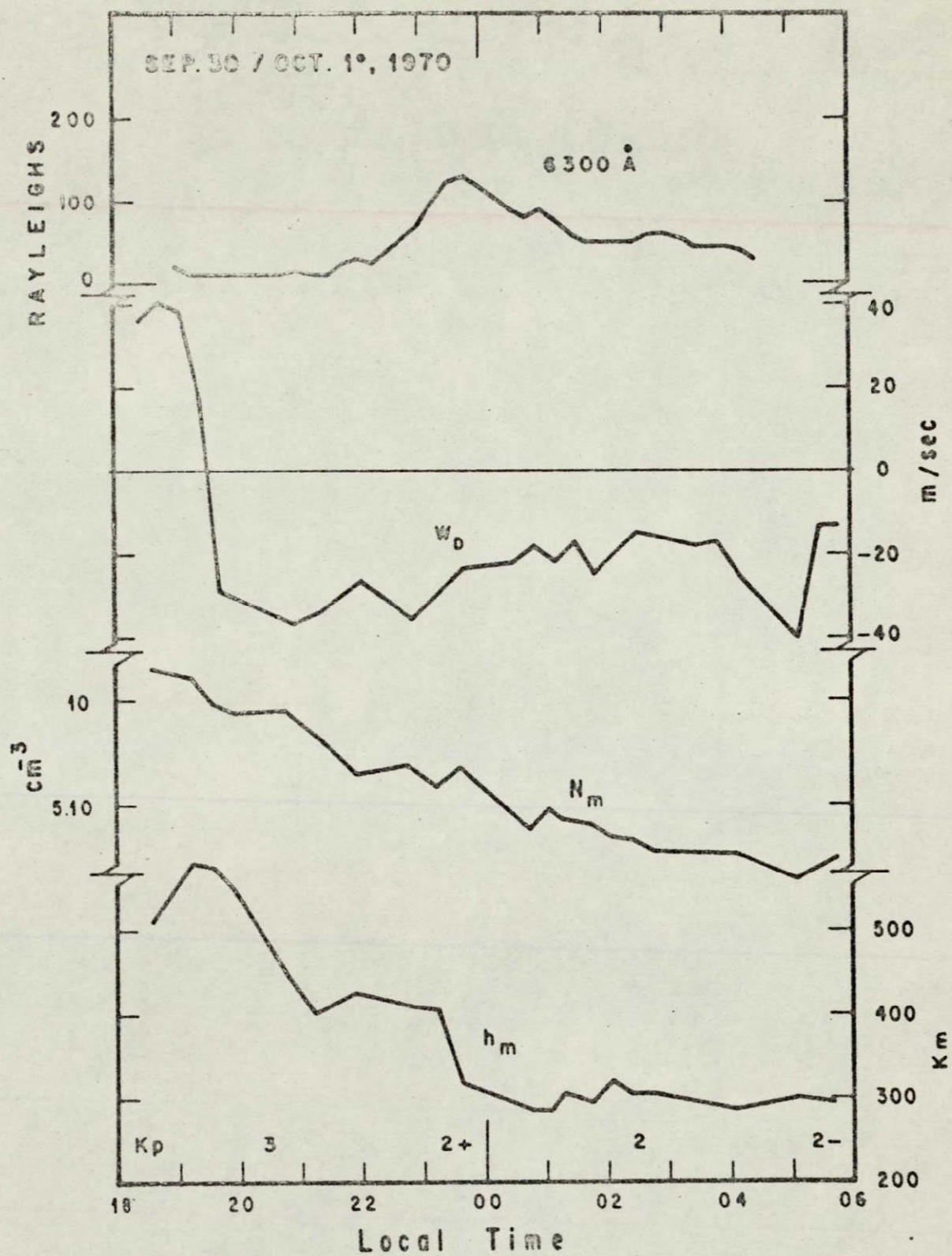


N°1659
JICAM.-2/Sep/70
P.L./slght.

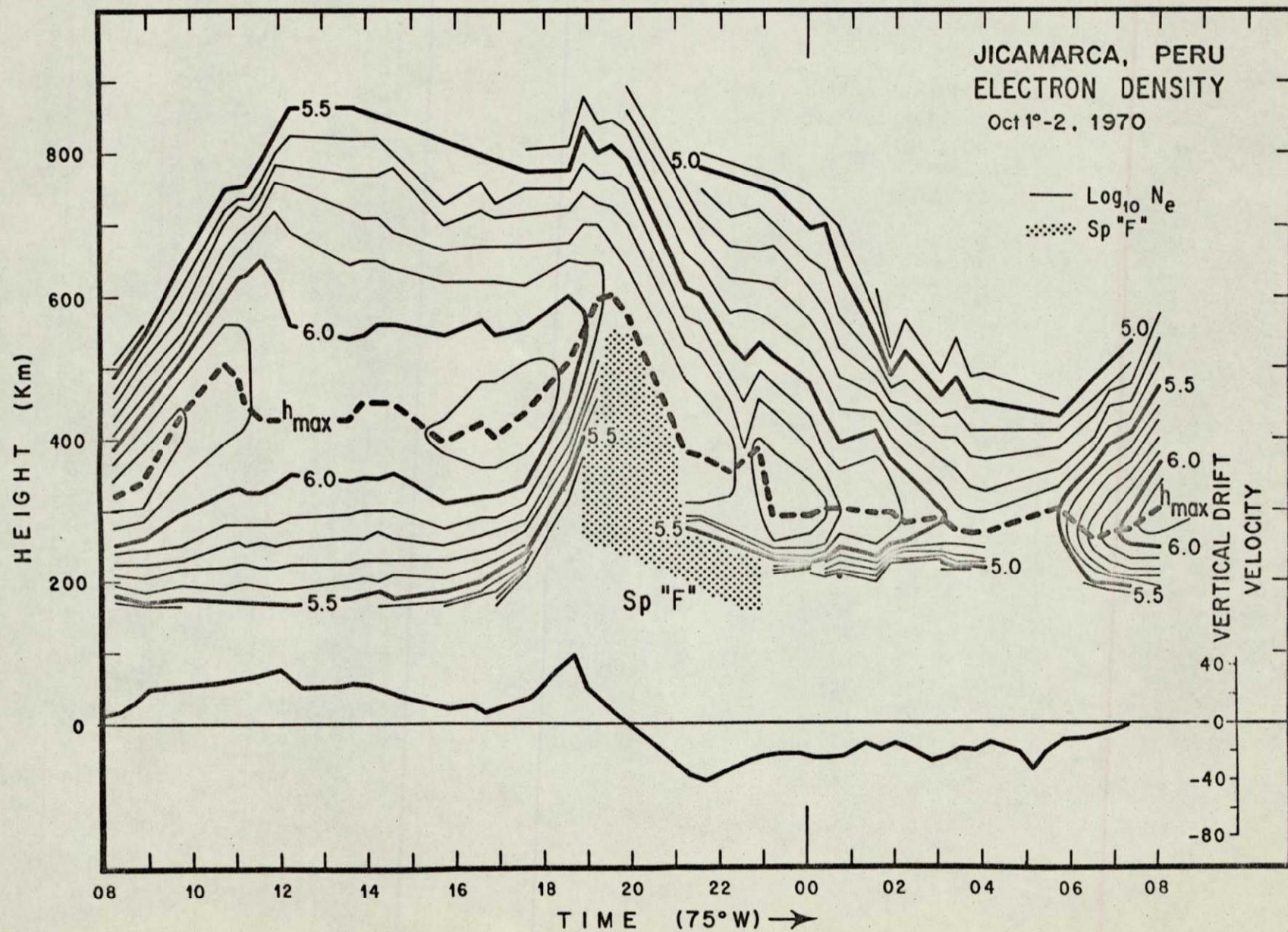


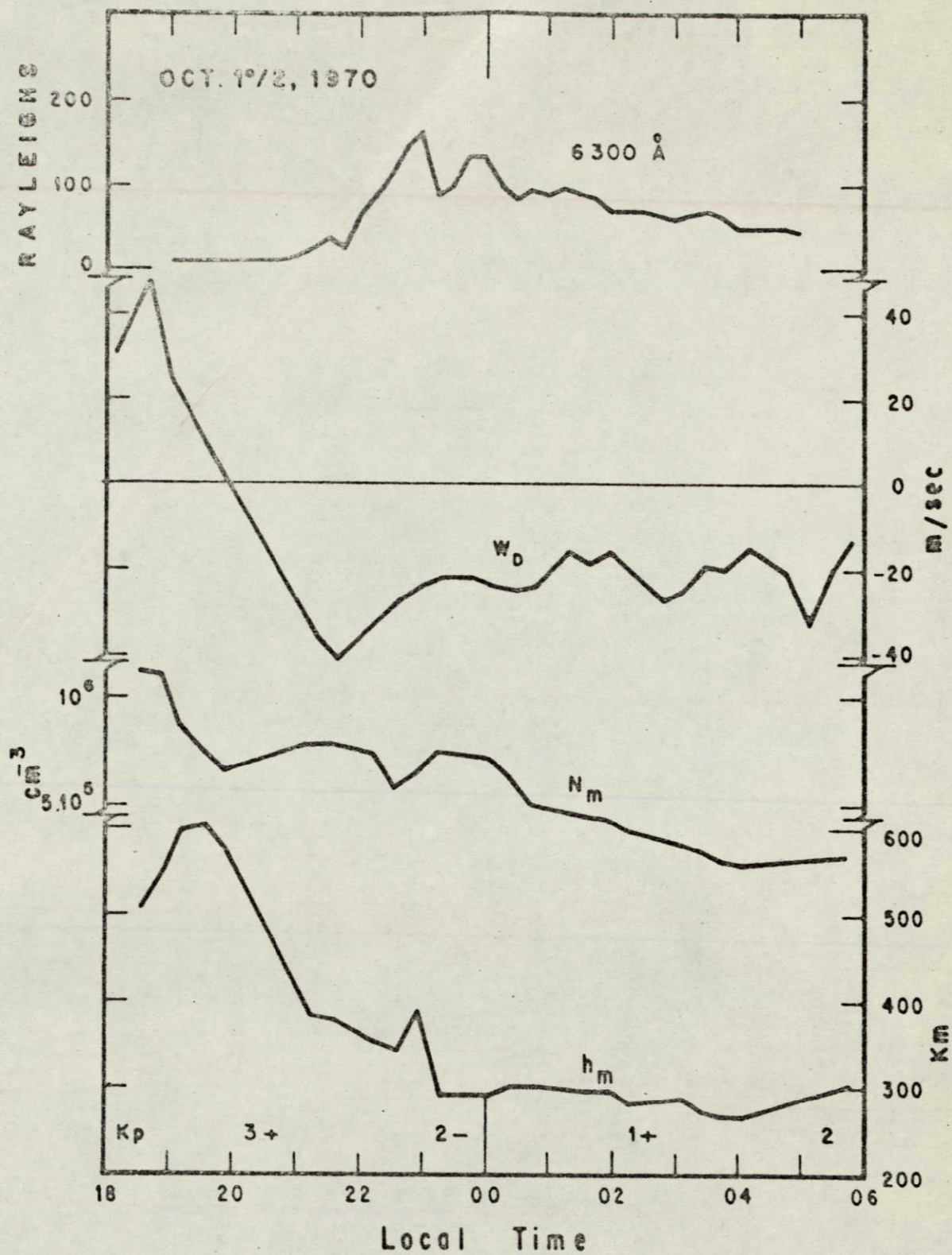






N°1762
JCAM - M/3er/71
P.L./sleht.





M*1784
JCAM-17/Mar/71
P.L./elekt.